Precision Engineering of Micrometer and Nanometer Droplets for Ultrasound Imaging and Therapy

Thomas D. Martz

A dissertation submitted to the faculty of the University of North Carolina at Chapel Hill and North Carolina State University at Raleigh in partial fulfillment of the requirements for the degree of Doctor of Philosophy in the Joint Department of Biomedical Engineering.

Chapel Hill
2011

Approved by:

Paul A. Dayton, Ph.D.

Robert Dennis, Ph.D.

Glenn Walker, Ph.D.

ABSTRACT

THOMAS D. MARTZ: Precision Engineering of Micrometer and Nanometer Droplets for Ultrasound Imaging and Therapy. (Under the direction of Paul A. Dayton, Ph.D.)

The medical community has interest in improving techniques such as occlusion, therapeutics and imaging through the use of liquid perfluorocarbon droplets. The ability to create a monodispersed population of liquid perfluorocarbon droplets would have the added advantage of uniform acoustic activation parameters. A microfluidic device with a flow-focusing orifice allowed for uniform production of perfluoropentane droplets in the micron and submicron diameter range. These droplets are able to be stored for over two weeks while retaining distribution characteristics. The observed activation of the droplets shows the acoustic threshold as a function of droplet diameter with little variability. Results showed that microfluidic technology with a pressure controlled flow regulator will allow for greater manufacturing control of phase-change perfluorocarbons in the micron and sub-micron size range for acoustic droplet vaporization applications.

ACKNOWLEDGMENTS

The author would first like to thank the committee for their time and effort throughout the thesis process: Dr. Paul A. Dayton, Dr. Bob Dennis and Dr. Glenn Walker. The author would also like to thank the Paul A. Dayton lab and Abraham P. Lee lab for their assistance and help with aspects of the research. The continual support from family has assisted the author to strive for the best results possible. This project was supported by The Richard Goolsby Scholarship, R01EB008733 and R21EB011704.

Contents

List of Figures

List of Tables

Chapter 1

Specific Aims

In the 1990s, the US Department of Defense supported programs that included the creation of field-deployable microfluidic devices for detecting biological threats. Since that time, the microfluidic process has evolved and rapidly advanced for use in a variety of applications(Whitesides, 2006). Microfluidic devices were initially made from glass and silicon. However, it was soon discovered that these materials did not encompass all of the material properties that were needed for success in microfluidics. Due to its near optical transparency and soft flexible elastomer, polydimethylsiloxane or PDMS became the most widely used material for microfluidic applications. Also, a notable advancement in the field, soft lithography, has made it possible to go from design to production in less than two days(Whitesides, 2006). With the evolvement of microfluidics, the ability to create controlled bubbles (Garstecki et al., 2004) and droplets (Whitesides, 2006) began to develop. For example, a flow-focusing device with a small pinch off area has been shown to create uniform droplets or microbubble samples (Garstecki et al., 2004). The evolution of microfluidics has given us the opportunity to create uniform droplets for applications such as contrast enhanced ultrasonography (Kripfgans et al., 2002; Marsh et al., 2007), vessel occlusion (Kripfgans et al., 2002; Kripfgans et al., 2005; Zhang et al., 2010), drug delivery (Rapoport et al., 2009b), or multi-purpose systems (Fabiilli et al., 2010b). These droplets can be fabricated in the micron and sub-micron diameter range. To the knowledge of the author, the uniform fabrication of sub-micron droplets or sub-micron acoustic droplet vaporization (ADV) agents, without a resulting large diameter droplet, is novel.

There are other means to create ADV vehicles such as mechanical agitation and sonication (Fabiilli et al., 2010b; Rapoport et al., 2010). Lipids and Perfluorocarbons (PFCs) are the most commonly used materials for ADV agents. Perfluoropentane

(PFP) was used exclusively in this research due to its boiling point (29°C) being close to physiological temperatures. At this boiling point, the introduction of an acoustic pressure from an ultrasound transducer, can induce a liquid to gas phase-change. An ultrasonic induced phase change of ADV vehicles may have many different applications including, but not limited to, controlled drug release , controlled vessel occlusion, and an increase in contrast enhancement. Prior to our research , the fundamental problems associated with ADV agent fabrication methods included vagueness in the activation threshold and the uncertainty of its use in ultrasound contrast enhanced applications based on phase-change bubble size. To address the needs of the medical ultrasonics field, we propose the following hypothesis:

Hypothesis: The development of size-controlled micron and sub-micron droplets for controlled vessel occlusion, drug delivery vehicles, and ultrasound contrast agents can be created and tested using rapid prototyping microfluidic devices .

To test this hypothesis, we propose the following Specific Aims:

1.1 Aim 1: Design a versatile microfluidic device to create a spectrum of droplet sizes with different materials.

- Vary the diameters of channels and orifices to maximize the efficiency of the microfluidic device. (UCI)
- Implement a notched output collection mechanism for easy collection.

1.2 Aim 2: Precisely control the input of the target reagents into the microfluidic device.

- Implement a pressure vessel to control the input flow of the reagents for an enhanced and prolonged control of the sample.

1.3 Aim 3: Create uniform/monodisperse micron and sub-micron samples.

- Introduce a pressure control flow system to improve the control of vehicle diameters.
- Demonstrate that the pressure control flow system can be used for "nano tip-streaming" and the production of sub-micron vehicles.

1.4 Aim 4: Initiate acoustic droplet vaporization to demonstrate controlled uniform activation and overall expansion.

- Create a system in which an ultrasound transducer is aligned with a microscope objective and the sample to visually show and record ADV.
- Incrementally increase the pressure of the ultrasound transducer to reach the ADV threshold.
- Characterize a variety of sizes and compositions to determine the droplet vaporization threshold of a given diameter droplet.

1.5 Aim 5: Show that the vehicles will maintain stability over time.

- Improved the lipid formulation to reduce coalescence and thus improve the longevity of the sample.
- Test the samples over a two week period to show that the vehicle population stayed uniform.

Chapter 2

Significance

2.1 Aim 1: Design a versatile microfluidic device to create a spectrum of droplet sizes with different materials.

"This research was a collaboration between UNC and UCI. Roger Shih and David Bardin were the main contributors in updating device designs and microfluidic wafer fabrication methods."

A versatile microfluidic device created with a rapid prototyping procedure will allow for a range of parameters to be tested cheaply and quickly. Other types of vehicle production methods incorporate a variety of materials that may take hours to complete. During that time, it is difficult to watch the production of the vehicles and subsequently control the vehicle size or population. Thus, a system needed to be created that would allow for no excess materials to be used, a real-time means of visualizing production, and the ability to alter the vehicle population in real time. A microfluidic device allows only the droplet materials to be introduced into the system. It is also optically transparent for real-time production visualization and minute changes to the input system of the device will allow for vehicle population control.

Early samples made with our microfluidic system created very delicate droplets that could not even reach the output without coalescing. Initial designs called for the output region of the microfluidic to have a cylinder shape in which material and droplets would collect and wait for transfer. This was found to alter the production of the microfluidic device over time based on how full the output cylinder was. Since this was added variation, the system had to be changed to aid in the pressure gradient and the ease

of collection. Cutting a wedge at the end of the sample solved the pressure gradient problem and it made collection easier. The wedge design did not hamper production of the device and the capillary forces of the lipid and vessels on the PDMS allowed for easy collection without having to alter the microscope setup.

2.2 Aim 2: Precisely control the input of the target reagents into the microfluidic device.

The input process of the reagents into the microfluidic device is directly related to the quality of the sample. Using syringe pumps, there may be a 10% variation in the mean diameter of the output sample (Korczyk et al., 2010). The large variations exacerbate the problems when samples are less than 20 µm in diameter. This amount of variation makes it difficult to control the population over a long enough time frame to produce a viable sample. Thus, a more sustainable input process is needed. It was found that using a pressure vessel with a precision regulator substantially decreased the amount of variation from the mean. This was a large enough improvement to create a sample, but the added advantage was that a sample could be altered from 20µm to 5µm in a matter of seconds and remain stable.

2.3 Aim 3: Create uniform/monodisperse micron and sub-micron samples.

Acoustic droplet vaporization is commonly shown with a polydispersed sample (Fabiilli et al., 2010b; Rapoport et al., 2010). This creates a variance in the acoustic threshold based on the size of the droplet population. If the distribution is wide, then a much higher acoustic pressure is needed to activate the population compared to a uniform sample. Also, there is the added complexity that a large droplet that is converted to a bubble with a low acoustic pressure could influence the remaining droplets' acoustic threshold creating further uncertainty. Microfluidics were introduced into the study in order to tailor the size distribution to a low polydispersity index. This paired with the pressure control flow system creates uniformity in samples ranging from 800 nm to 25µm.

2.4 Aim 4: Initiate acoustic droplet vaporization to demonstrate controlled uniform activation and overall expansion.

PFP droplets have been shown to be slightly echogenic (Kripfgans et al., 2002; Marsh et al., 2007) but a PFP gas bubble has shown to be highly echogenic within a given system. The samples would not be useful unless they were susceptible to ADV. The samples created were able to be converted to a bubble with a size-dependent acoustic pressure. After droplets were activated via vaporization, the echogenicity of the resulting bubbles would allow for applications such as perfusion mapping. Droplet vaporization also makes drug delivery possible as this allows the drug to be housed within the droplet shell protected from its surroundings or coated and attached to the outside of the shell. Upon activation, the drug would be released at site-specific targets to reduce systemic toxicity. Embolotherapy is also possible as the theoretic expansion rate of the droplet is approximately 6 times the initial diameter. Reducing the blood flow of a site-specific area to a high degree could lead to ischemic necrosis (Kripfgans et al., 2005). There have also been cases where occlusion is paired with drug delivery in the effort to increase the residence time of the chemotherapeutic in the target area.

2.5 Aim 5: Show that the vehicles will maintain stability over time.

Initial droplets were unable to be transferred from the microfluidic device to a storage container. This would make the samples unusable for any type of scale-up applications. The formulation of the lipid composition was allowing the droplets to coalesce or burst. This caused the lipid reagent to be reformulated twice in order to achieve a droplet population that has the ability to last for at least two weeks. The idea behind keeping the samples refrigerated for two weeks was so that these samples could be made in a laboratory, shipped to the user, and sit until final use. During this time frame, the droplet population should maintain a similar distribution for continuity. Overall, the sample has to last long enough to use it and the reformulated lipid reagent allows for easy handling, use and longevity of the vehicles.

Chapter 3

Innovation

3.1 Aim 1. Design a versatile microfluidic device to create a spectrum of droplet sizes with different materials.

"This research was a collaboration between UNC and UCI. Roger Shih and David Bardin were the main contributors in updating device designs and microfluidic wafer fabrication methods."

With the creation of the initial microfluidic device, it became possible to go from design to use in less than two days (Whitesides, 2006). Also, with the addition of the flow focusing device, two or more materials could be introduced into a flow-focusing device to create a variety of samples including multi-layer vehicles (Hettiarachchi et al., 2009), ADV agents (Martz et al., 2011; Sheeran, 2011; Sheeran et al., 2011b; Sheeran et al., 2011a), and Janus particles (Malloggi et al., 2010). The innovation of the microfluidic device is in the ability to pattern a 6 micron-orifice to allow for balance in production between sub-micron sizes and micron sizes. Another improvement is the addition of a complex filtering system, which stops the device from clogging. In normal circumstances, the fabrication technique can produce objects that are larger than 6 microns, which halted production of droplets. The filtering system evolved over the duration of this research to allow for upwards of 60 psi to be placed on the reagents to induce flow without the fear of clogging.

In relation to sample collection, an initial problem was the large bulk output hole. This large hole created a pressure gradient over time depending on the amount of droplets and excess lipid at any given time. This pressure gradient created instabilities

in the production of the droplets leading to samples with a nonuniform distribution. In an attempt to stabilize production, Tygon tubing was placed into the output hole to allow the material to flow into a collection vessel. Unfortunately, droplets sink in a lipid medium and in our method, the droplets were required to go up a slight slope before they could be collected in the vessel. Therefore, the droplets had to build up before moving into the collection vessel, which ultimately led to the previously described pressure gradient. The innovation came with the introduction of a "V" shaped slice in the output of the device where capillary forces act at the PDMS and glass interface to allow for easy collection of the droplets with minor lipid waste.

3.2 Aim 2. Precisely control the input of the target reagents into the microfluidic device.

Initially, to create multi-layered acoustically active liposomes, four syringe pumps were used for the introduction of reagents. ADV agent research required just two materials, thus we were able to reduce the overall number of syringe pumps to two. Syringe pumps were used as a controllable method for the introduction of the reagents into the microfluidic device due to their ability to maintain hysteresis over a duration of time when the flow rate was changed. However, there was play between the syringe pump and the syringe holding the reagent, the use of a plastic syringe induced flexibility to the chamber complicating the fluidity of the reagent flow, and the syringe pumps did not allow for precise control of the reagent flow that is required to create uniform ADV agents. These issues led to the initiation of a new method for introducing the reagents.

The innovation in this research was the use of a pressure control flow system to introduce the reagents into the microfluidic device. A constant and instantly updatable pressure head was placed on the top of the reagent in a pressure vessel. A line submerged in the reagent equalized the pressure by sending the reagent to the microfluidic device initiating flow. Although not personally studied, the initial knowledge for this design showed that there was less than 1% variation of the mean diameter of droplets overtime (Korczyk et al., 2010). This advancement allowed for more uniform droplet production and diameter variation from sub-micron droplets to micron droplets in a matter of seconds.

3.3 Aim 3: Create uniform/monodisperse micron and sub-micron samples.

Initial microfluidic designs utilized an orifice larger than 10 microns. This prevented many of the smaller size samples from being produced due to geometric constraints and the inability to control the flow of the reagents precisely. The innovation of a smaller orifice (6 microns patterned), along with the ability to precisely control the flow of reagents with a pressure vessel, has allowed the effortless production of monodisperse micron sized droplets and the uniform production of sub-micron droplets.

Droplets were created with the use of syringe pumps during the initial studies of this research. This required 100% focus on the device screen to ensure that the droplets did not vary and the uniformity of the sample was not compromised. The innovation of the pressure control flow system to create the uniform samples was the breakthrough that was needed for stable sample creation. With the new pressure control flow system, there is an instant update of droplet size based on the input pressures, the ability to perform nano tip-streaming to produce sub-micron droplets, and the ability to leave the system for hours to produce bulk samples without the fear of variation from the initial droplet diameter. According to a recent literature search, this microfluidic device is the first to create sub-micron droplets with the capability to achieve ∼300nm.

3.4 Aim 4: Initiate acoustic droplet vaporization to demonstrate controlled activation and overall expansion.

Initially, the fabricated droplets coalesced over time. Thus, it would take less pressure to activate the droplets, thereby disrupting the actual activation threshold of the correct size droplets. This was also compounded with the initial problems of droplet collection, which resulted in an increase in droplet coalescence and a wider distribution of droplet diameters. The innovation was a joint effort between an improved lipid formulation, pressure control flow system, and "V" collection method. These allowed for uniform sub-micron and micron droplets to be produced consistently over time to produce a viable sample without coalescence of resulting droplets, and thus providing an easy collection for implementation into the ultrasound testing apparatus.

3.5 Aim 5: Show that the vehicles will maintain stability over time.

Initial droplets were produced with a pure lipid solution that allowed droplets to coalesce into sizes outside the spectrum of the research before they could even be collected. The lipid solution was reformulated adding surfactant and glycerol, which prevented the droplets from coalescing over time and from the weight of other droplets. With the innovation of an equal ratio of lipid to surfactant to glycerol, coalescence was avoided and allowed the samples diameter distribution to stay relevant over an industrially applicable time.

Chapter 4

Materials & Methods

4.1 Materials Database

Process	Material	Company	Location
Reagents	Liquid Perfluoropentane	FluoroMed	Round Rock, TX
	1,2-distearoyl-sn-glycero-3-phosphocholine	Avanti Polar Lipids	Alabaster, AL
	1,2-distearoyl-sn-glycero-3-phosphoethanolamine-	Avanti Polar Lipids	Alabaster, AL
	N[methoxy-(polyethylene glycol)-2000]		
	Deionized Water	-	-
	Glycerol	Fisher Scientific	Pittsburgh, PA
	Proplyene Glycol	Fisher Scientific	Pittsburgh, PA
	Pluronic F-68	Sigma-Aldrich Corporation	St. Louis, MO
	Chloroform	Fisher Scientific	Pittsburgh, PA
	Nitrogen Gas	AirGas	Charlotte, NC
Microfluidic Device	Illustrator	Adobe	San Jose, CA
	Mask	CAD/Art Services	Brandon, OR
	SU-8-25 UV Curable Epoxy	MicroChem	Newton, MA
	Polydimethylsiloxane	Dow Corning	Midland, MI
	PDMS Curing Agent	Dow Corning	Midland, MI
	2947-75X25 Microscope slides	Corning	Corning, NY
	Plasma Cleaner	Harrick Plasma	Ithica, NY
Droplet Production	Olympus 1X71 Inverted Microscope	Olympus	Center Valley, PA
	50x objective	Olympus	Center Valley, PA
	Fastcam APX-RS	Photron, Inc.	San Diego, CA
	Tygon S-54-HL tubing	Saint-Gobain Performance Plastics	Akron, OH
	Syringe Pumps	Harvard Apparatus	Harvard, MA
	Syringes	BD	Franklin Lakes, NJ
	3 mL Serum Vial	Wheaton	Millville, NJ
	Caps	Wheaton	Millville, NJ
	Septa	Wheaton	Millville, NJ
	Pressure Gauges	SPAN Instruments Inc.	Plano, TX
	Precision Pressure Regulator	Airtrol Components, Inc.	New Berlin, WI
Acoustic Testing	Olympus 1X71 Inverted Microscope	Olympus	Center Valley, PA
	Microcellulose Tubing	Spectrum Labs, Inc.	Greensboro, NC
	5 MHz Piston Transducer	Valpey Fisher Corp.	Hopkinton, MA
	100x water immersion microscope objective	Olympus	Center Valley, PA
	HNA-0400 needle-hydrophone	Onda Corp.	Sunnyvale, CA
	Waveform Generator	Tektronix	Beaverton, OR
Analysis	Image J	NIH	Bethesda, MD
	Calibrated Reticle	Edmund Industrial Optics	Barrington, NJ
	AccuSizer 780A	Particle Sizing System	Santa Barbara, CA
	Malvern Nano ZetaSizer	Malvern Instruments Ltd.	Worcestershire, UK

Table 4.1: Materials Used During Research

4.2 Microfluidic Device Fabrication

"This research was a collaboration between UNC and UCI. Roger Shih and David Bardin were the main contributors in updating device designs and microfluidic wafer fabrication methods."

Initial flow-focusing channel designs were created in Adobe Illustrator. The basic layout of the design is pictured in figure 4.1. There are two input holes located on the device with one larger output hole. The design strategy surrounding the flow focusing device is that the outside input hole (lipid) branches to a "T" as illustrated. This "T" branching is brought around the second input hole (PFP) to create a sandwich of lipid/PFP/lipid. This sandwich is located at the flow-focusing region in a pinched orifice that was patterned to be approximately 6 µm. After the orifice, there is an arrow shaped output channel that leads to the output orifice.

The design in Adobe Illustrator was printed at 20,000 dpi by CAD/Art Service and subsequently used as the mask for the silicon wafer. This silicon wafer was first oxidized with the use of a plasma cleaner and spin-coated with a UV curable photoresist. The printed mask was then aligned to the wafer using alignment markers.The wafer was exposed to UV light to develop the channel patterns for use as a negative for device production. The negatively patterned device was then secured in a Petri dish.

Polydimethylsiloxane (PDMS) and a curing agent were placed into a measuring cup in a 10:1 ratio. These materials were mixed resulting in a thick solution containing many small bubbles. The entire contents were then poured over the silicon wafer in the Petri dish. The thickness of the device was a minimum of 1 cm. The Petri dish was then transferred to a vacuum for at least 3 hours to remove any bubbles. A light nitrogen blast helped to remove any residual bubbles that remained in the device area. Lastly, the Petri dish was placed in an oven at 60°C for a minimum of 5 hours to complete the PDMS curing process.

The remaining steps for microfluidic device production were performed in a laminar flow hood. To assist in the removal process, the devices were cut from the PDMS when the PDMS was still warm from the oven. A syringe was used to create a circular cut in the PDMS just inside the outside diameter of the silicon wafer. The circular piece of PDMS was then removed and a razor blade was then used to separate the individual devices.

Individual devices remained inverted in the hood at all times to avoid dust or contaminants. A blunt tip needle was used to remove the PDMS located over the two

input hole regions approximately the size of the Tygon tubing. A razor blade was then used to cut a triangle shape that extends off the device at the output location. The surface and holes were cleaned out with ethyl alcohol and dried with a nitrogen gun. Then, a glass slide was cleaned with ethyl alcohol dried with a nitrogen gun. Care was taken to ensure that there was no residue or debris on the glass slide, which would potentially lead to device failure. The microfluidic channels and glass slide were then placed in a plasma cleaner on high at 500 millitorr for 3 minutes. The microfluidic channels and glass were immediately joined together and held together for at least 30 seconds to ensure a secure bond. Finally, the device channels were filled with DI water and sealed with a piece of scotch tape.

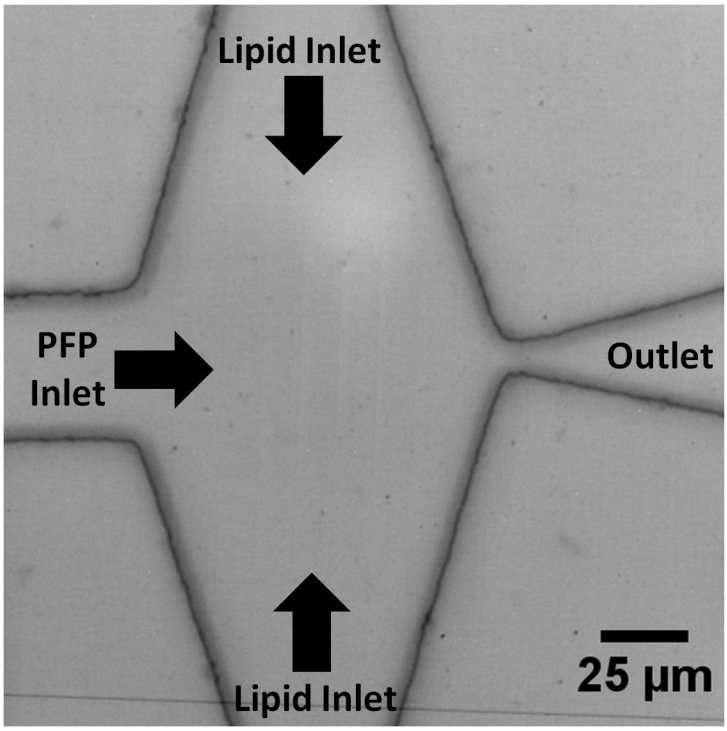

Figure 4.1: Microfluidic Device Layout

4.3 Reagent Preparation

PFP was kept sealed after transfer to ensure the PFP did not evaporate. Initial lipid was created using chloroform to dissolve a 9:1 molar ratio of 1,2-distearoyl-snglycero-3-

phosphocholine (DSPC) and 1,2-distearoyl-sn-glycero-3-phosphoethanolamine-N[methoxy-(polyethylene glycol)-2000] (DSPE-PEG2000). The chloroform was subsequently evaporated with the use of a nitrogen gun. For the two lipid compositions used in this research, DI water was added as the base for the lipid solutions. The first lipid composition included the addition of 50 mL of DI water and was sonicated for 20 minutes. After this, 47 mL of DI water was added along with 2 mL of glycerol, 1 mL of propylene glycol, and 10 mL of pluronic F-68 surfactant. Finally, this was vortex mixed for 1 minute and sonicated for 10 minutes. This was then used as the lipid reagent for droplet production. The second lipid composition was created with the base ratio as previously stated. 1 mL of the lipid composition was added to 1 mL of glycerol, and 1 mL of pluronic F-68. This solution was then lightly vortex mixed until the appearance of a homogeneous solution. This was then used as the lipid reagent for droplet production.

4.4 Reagent Flow Control

Initial studies were performed with the use of two syringe pumps. These pumps were placed on stages to ensure that the syringe height was located at the height of the microfluidic device. A 5 mL syringe was used as the lipid container and the PFP was housed in a 3 mL syringe. The syringes had a needle at the output that was connected to Tygon tubing, which ran to the microfluidic device inputs. Pressure vessels were used for the remainder of the research due to our need to precisely control the fluid flow. 3 mL of PFP were placed in a 3 mL serum vial. This vial was then capped. Also, 3 mL of lipid reagent was placed in a 3 mL serum vial. This vial was also capped. The septa that were used to cap the vials had two holes placed in them that were slightly smaller than that of the Tygon tubing. A strand of Tygon tubing was placed in each hole. One strand in the headspace of the vial went to a precision pressure controller. This pressure controller was also connected to a pressure gauge as well as an output hole. This output hole contained rigid tubing that ran to a Nitrogen tank. The Tygon tubing submerged in the given reagent went directly to the input hole of the microfluidic device. The two reagents were then able to be precisely pressure controlled to receive the desired flow rates thus producing the desired droplets.

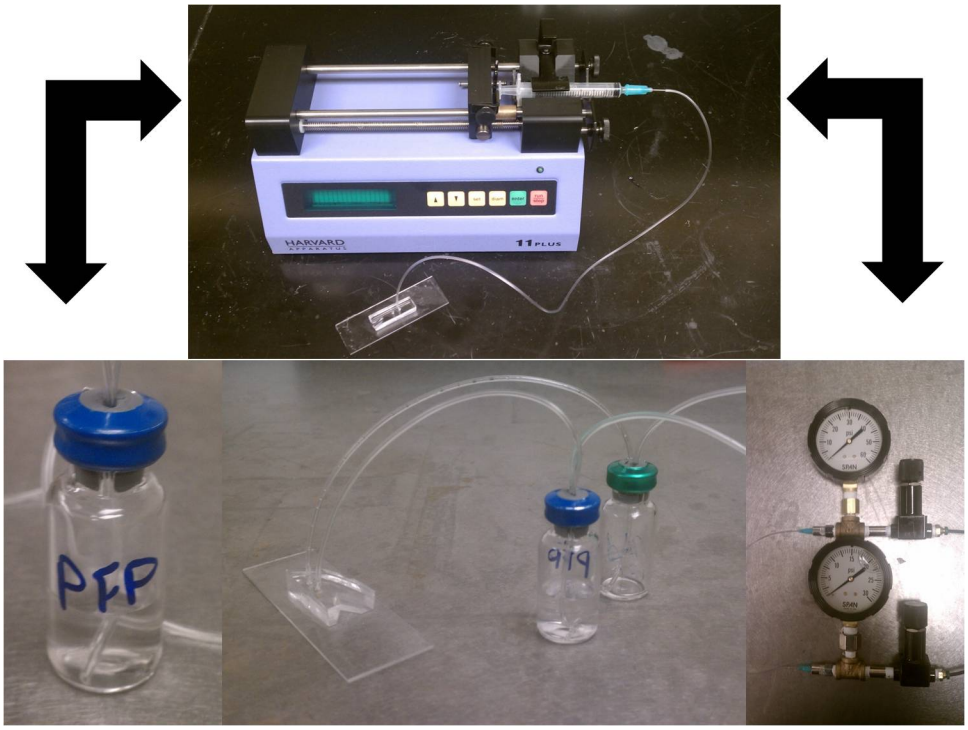

Figure 4.2: Syringe Pump System and the Pressure Control Flow System

4.5 Microfluidic Droplet Production

The microfluidic devices were placed into a custom made holder on the top of a 2D adjustable stage on an inverted microscope. The microfluidic device was then brought into focus with a 50x objective. A high-speed camera was connected to the microscope for video recording purposes. The amount of light was adjusted to create the proper brightness for video collection. A variety of different frame speeds and shutter speeds were used to record droplet production videos.

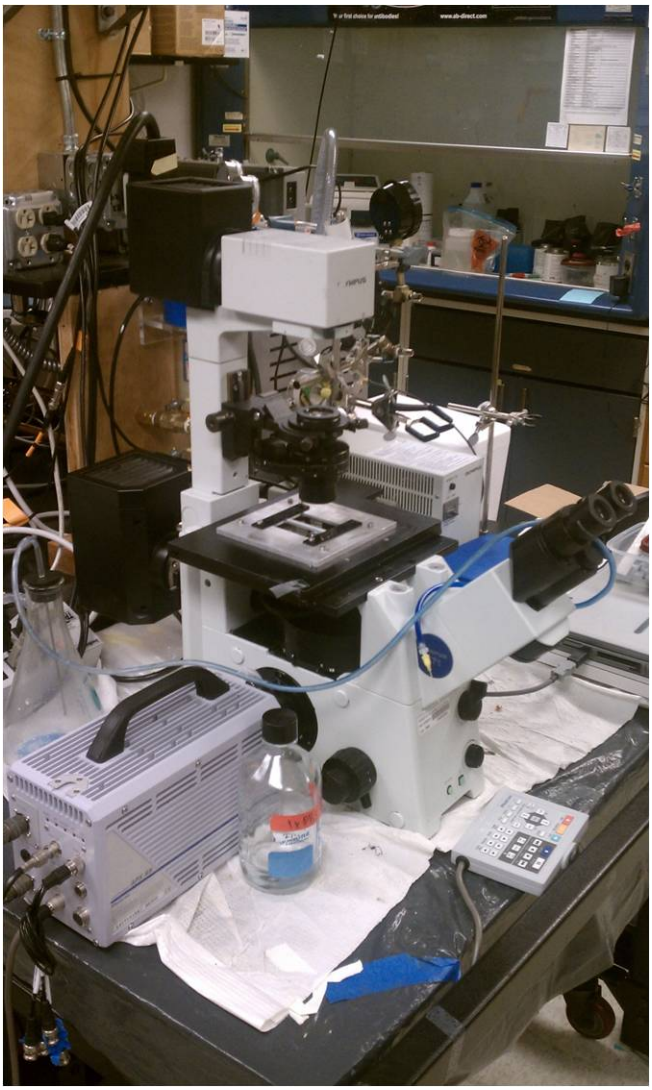

Figure 4.3: Microfluidic Device Testing Setup

4.6 Sample Collection

Droplets emerged from the output triangle along with excess lipid. A 1 mL pipetter set at 250 µm was placed at the edge of the PDMS and glass. The droplets and excess lipid were then captured and pipetted into a 3 mL serum vial. On completion of the sample collection, the vial was capped and placed in a refrigerator at 4°C.

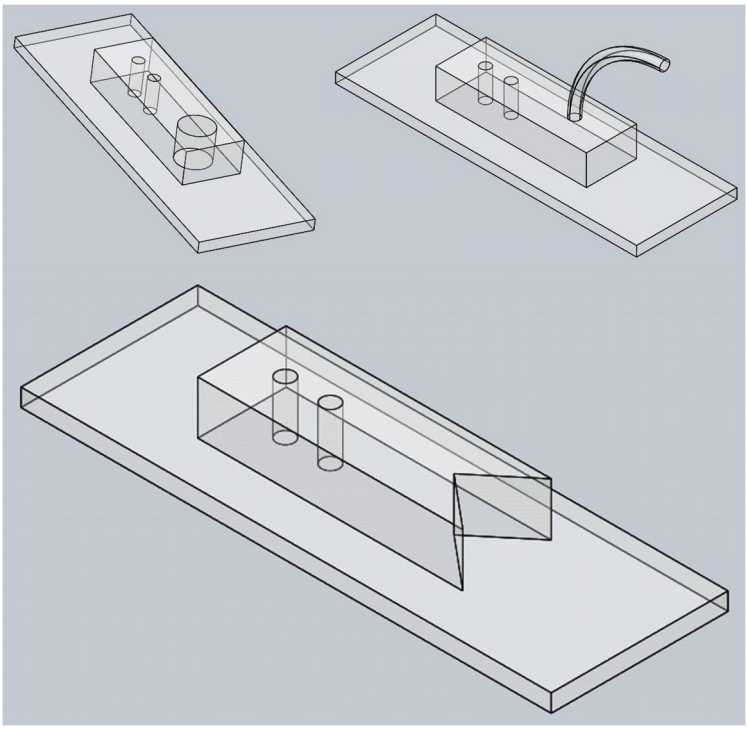

Figure 4.4: Microfluidic Droplet Collection Methods

4.7 Acoustic Droplet Vaporization

A heated water bath was placed on an inverted microscope with a 100x water immersion objective. A hydrophone was placed in the focused region of the microscope until the tip was visible. A transducer was submerged in the water bath and focused to the hydrophone which was also in the focus of the microscope. Then, the hydrophone was removed and a cellulose testing tube was placed in the optical focus. A cellulose testing tube was made with a brass "U" shaped rod, Tygon tubing, and a small amount of cellulose tubing. Tygon tubing was hot glued to one side of the brass rod. A piece of cellulose tubing was then glued into the Tygon tubing. The cellulose tube was then hydrated and another piece of Tygon tubing was glued to the cellulose tubing. The piece of Tygon tubing was then glued to the other side of the brass rod creating a tight area of cellulose tubing in the "U" of the brass rod.

The sample was then precisely input into the tube to focus on individual or groups of droplets. The input pulse was a single cycle, which was ramped up in pressure until

the droplet was activated to a gas bubble. Video was taken before and after activation with the use of a high-speed camera.

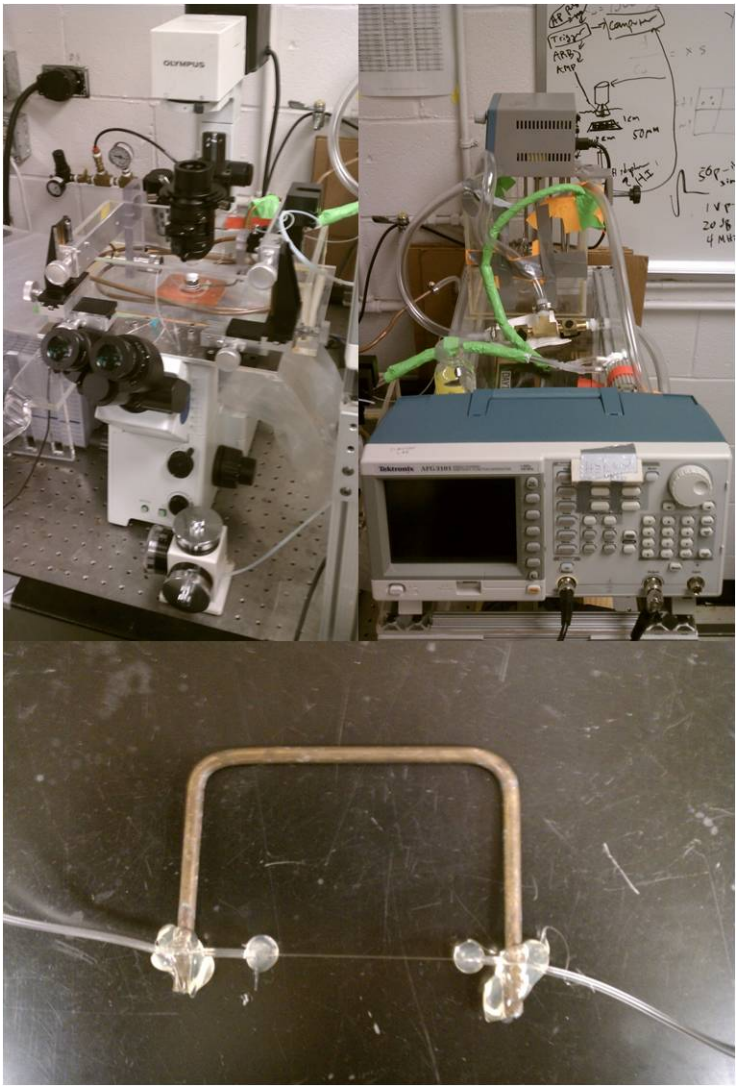

Figure 4.5: Acoustic Droplet Vaporization Testing Setup

4.8 Sample Processing

Image J was used to analyze the diameter of the droplets produced in the microfluidic device and the droplets before activation. A microscope reticle was used for

distance calibration of the video images. Production rates were determined by counting the amount of droplets that passed a given distance on the video in a set time provided by the high-speed camera. Populations of data were imported into Excel for data processing.

Sub-micron bulk samples were analyzed using a Malvern Nano ZS. This allowed determination of the mean and the standard deviation of the droplet populations. An aliquot of sample was pipetted into a a cuvette along with 0.5 mL of phosphate buffered saline. To image the sub-micron droplets a negative staining TEM procedure was used. Samples were applied to a grid, stained with 1 % uranyl acetate and then imaged in the TEM.

Chapter 5

Results

5.1 Aim 1: Design a versatile microfluidic device to create a spectrum of droplet sizes with different materials.

"This research was a collaboration between UNC and UCI. Roger Shih and David Bardin were the main contributors in updating device designs and microfluidic wafer fabrication methods."

The microfluidic device that was used in this experiment was modeled from a previous study. This initial design contained no filtering and contained a large 20 µm orifice. Design iterations on this initial design yielded a much smaller orifice to create smaller samples. The first design contained diagonal slits to filter unwanted material from moving downstream to the orifice that was approximately 10 µm in width. From this, initial droplets were able to be created and vaporized, but they were not in the desired size range for medical ultrasonics (< 7 µm). In order to get the droplets smaller, the design was changed to include a triangular shaped obstacle pattern for enhanced filtering and the orifice was decreased to approximately 6 µm. This design yielded droplets in the size range required, <7 µm. Furthermore, the filtering system along with the pressure control flow system, allowed for the production of sub-micron droplets.

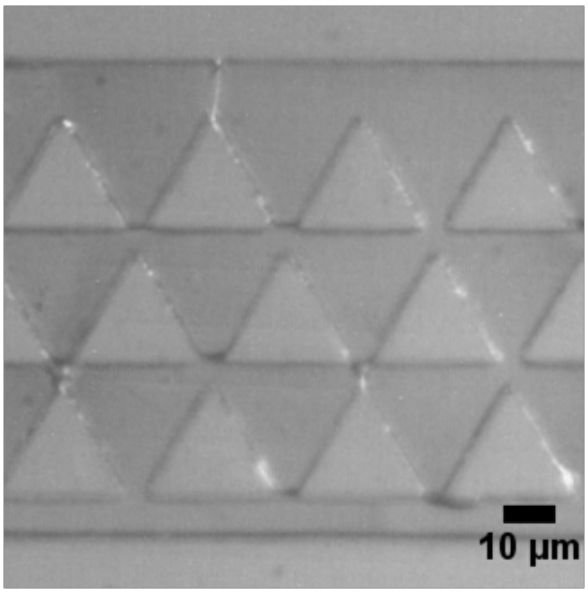

Figure 5.1: Microfluidic Device Filter System

A difficulty in collecting the droplet sample was having to move the light source away from the microfluidic device in order to remove the sample. Also, upon placing the sample in a collection vial, numerous droplets were vaporized due to pressure changes when they were output from the pipette. When the light source was away from the microfluidic device, it was not possible to watch the sample being created and on numerous occasions the droplet diameter changed by the time the light source was placed back on the microfluidic device. The fluctuation of fluid in the microfluidic device output also caused fluctuations as this attributed to the difference in droplet diameter when the light source was placed back on the microfluidic device. The first attempt to fix this was to place a piece of Tygon tubing in the output straight to the collection vessel. This appeared to fix the pressure gradient that was based on the amount of fluid in the output orifice but created a height differential that the droplets had to scale before they could be placed in the collection vessel. In an attempt to circumvent this problem, a wedge design was cut into the exit orifice for sample collection, which allowed easy access for the pipette to collect the sample as the light source remained on the device. The pressure gradient at the output was also stabilized as there was freedom for the output fluid and droplets to escape the device. Surface chemistry also played a role causing the output fluid and droplets to nest in at the boundary between the PDMS and glass.

Figure 5.2: "V" Shape Collection System

5.2 Aim 2: Precisely control the input of the target reagents into the microfluidic device.

Initially, two syringe pumps were used. Unfortunately, this particular setup made it difficult to simultaneously control two syringe pumps, especially with the low viscosity PFP in a horizontal syringe. Initial thoughts by the author were that the syringe pumps maintained a lot of give in relation to the plastic syringe holding the reagent and that the system would not stay stable even after an adequate soak time. This created samples with a lot of size variation. Korczyk et al.(Korczyk et al., 2010) showed that

there was a large amount of variation with syringe pumps and offered a simple low cost alternative. The basic design used a pressure vessel with an input and output. This design was used as the basis for the pressure control flow system shown here. The pressure control flow system ensured that only small amounts of material needed to be used, allowed for effortless control of reagent flow, and the eventual creation of sub-micron droplets.

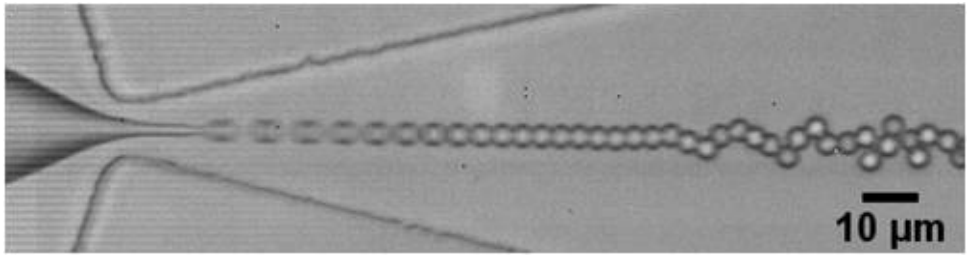

Figure 5.3: Consistent Monodispersed Droplet Production

5.3 Aim 3: Create uniform/monodisperse micron and sub-micron samples.

Numerous systems have to be in harmony to allow uniform/monodispersed micron samples to be created, not to mention sub-micron droplets. The microfluidic device has to be free of debris, sealed to the glass slide to ensure there are no breaks in geometry and resist flexing at higher pressures. The reagents have to be homogeneous, prevent coalescence once the droplets are created and have the ability to be collected. The pressure control flow system has to have a consistent amount of pressure applied to the reagents to ensure reliable flow rates and be easily controlled to alter droplet diameter. To allow uniform/monodispersed micron and sub-micron droplets, the microfluidic device went through two iterations, the lipid formulation was altered twice and pressure control flow system needed to be created.

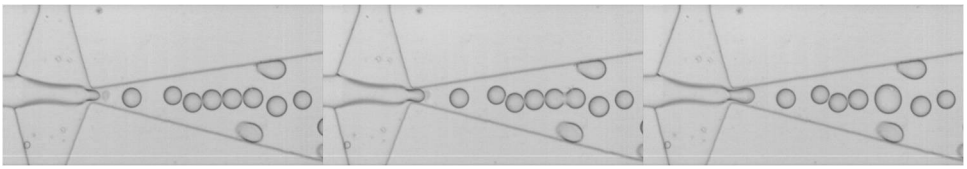

Figure 5.4: Initial Coalescence

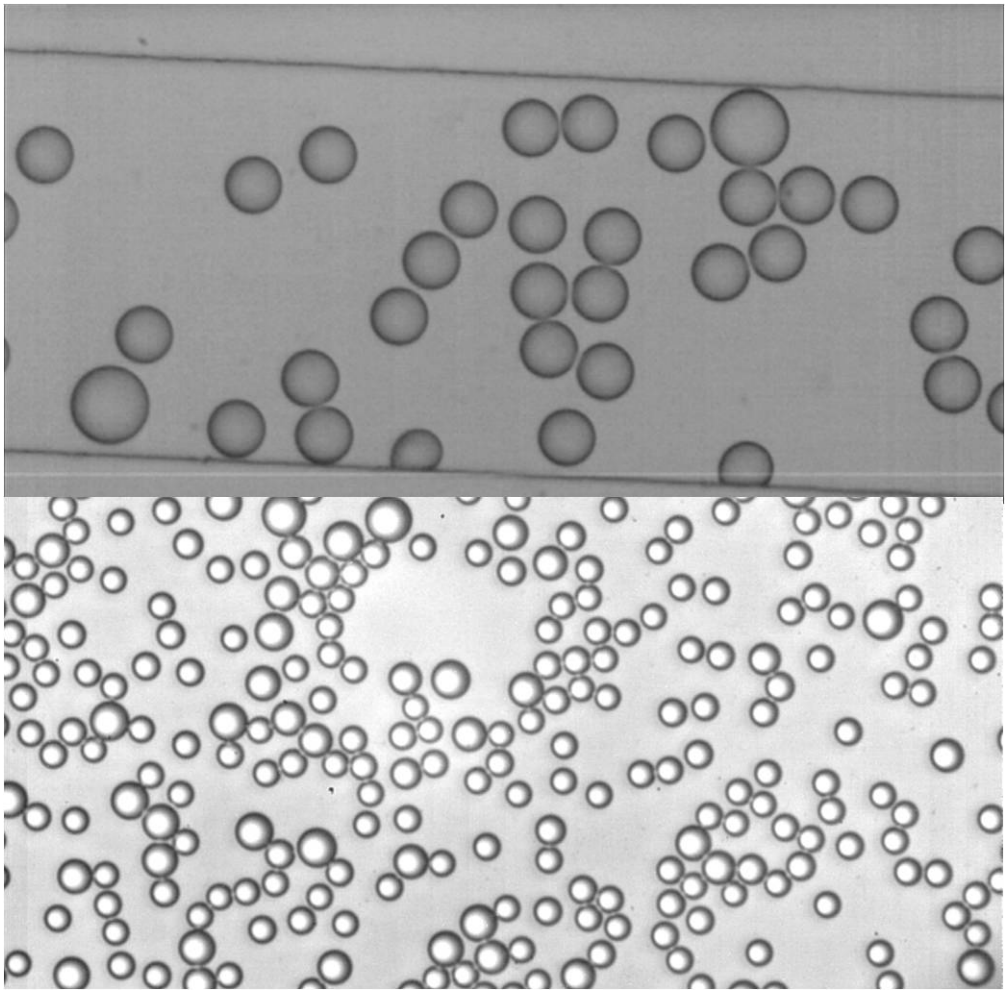

Figure 5.5: Initial Population Distributions

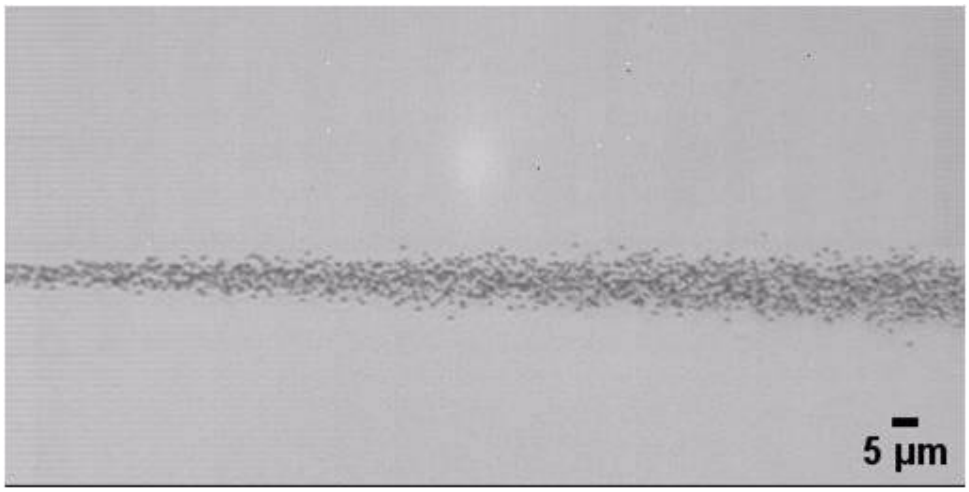

Figure 5.6: Uniform Sub-micron Droplet Production

5.4 Aim 4: Initiate acoustic droplet vaporization to demonstrate controlled activation and overall expansion.

Initial droplets created with the microfluidic system could not be removed from the microfluidic device to be placed in the acoustic testing apparatus. Iterations of the lipid composition were changed as well as the collection strategy that allowed the droplets to be administered into the acoustic testing apparatus. This then allowed a 5 MHz and 3.5 MHz transducer to administer a pressure pulse. Numerous droplet diameters were tested to determine that there is a discrete acoustic threshold for each diameter faction. Also, the activation threshold followed a logarithmic trend that shows the acoustic threshold increases as diameter decreased.

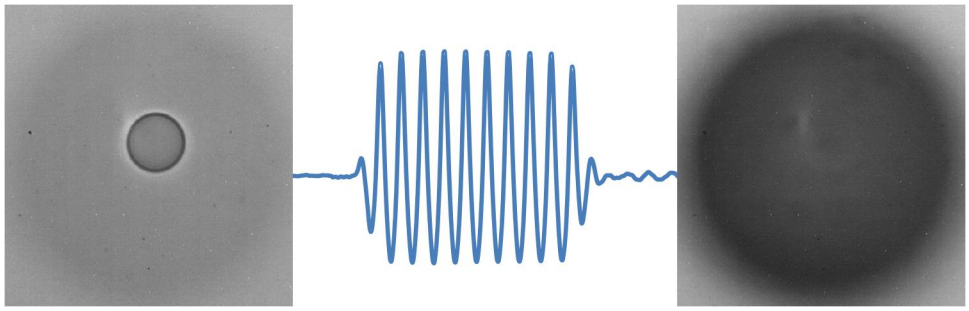

Figure 5.7: Acoustic Droplet Vaporization

5.5 Aim 5: Show that the vehicles will maintain stability over time.

To reiterate, the initial droplets created during this study were unable to be removed from the microfluidic device, which meant that they were not stable enough to last for an applicable time frame. This caused two iterations of lipid compositions to be created and a wedge collection style to be implemented. This allowed samples to be tested at incremental times through the span of two weeks. The results showed that the droplet diameters maintained a similar size and distribution compared to the day they were created. This then correlated to the droplets lasting an industrially applicable time frame similar to creation, shipping, storage, and medical use.

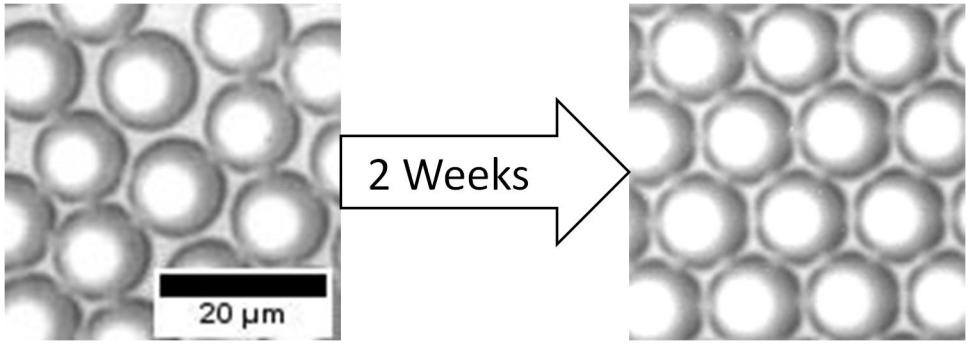

Figure 5.8: Stability of Droplets over 2 Weeks

Chapter 6

Results

The work presented here shows how improvement in different areas of the project culminated in the advancement of the ADV agent field. Microfluidic changes, reagent optimization, flow delivery mechanism and collection protocol all played a major role in the overall success of the project.

Microfluidics have allowed for the creation of monodispersed ADV agents. The initial microfluidic device was overhauled to allow for a smaller orifice and superior debris filters. The advancement in the microfluidic design allowed for progressively smaller droplets. Initial droplets were created with a diameter that was approximately 20 µm. The finalized design, on the other hand, produced droplet diameters that were ∼7 µm.

The reagent optimization was directly related to the overall population variation and the ability to collect the sample. Initial samples, regardless of creation diameter, would coalesce in the output of the microfluidic device resulting in a higher standard deviation. After creation of the final lipid composition, there was a drastic decrease in coalescence that improved the standard deviations of the output samples.In addition, it allowed for smaller droplet creation and easier collection. Syringe pumps have become common place when it comes to introducing reagents into a microfluidic device. In many cases, the ability to precisely control the flow over time is not necessary. However, in the application of fabricating monodispersed ADV agents, precise control is a necessity.

Syringe pumps were used initially in this study, but it became evident early on that they were not precise enough to maintain a constant diameter. Many days were spent using coarse pressure adjustments to compensate for lack of precision. This led to the creation of a pressure control flow system. The system had the ability to accurately control the production diameter of the sample and maintain that diameter over

a necessary amount of time for sample collection. The pressure control flow system also allowed for the introduction of the term "nano tip-streaming". This type of microfluidic droplet production enabled sub-micron droplets to be created.

Finally, the sample had to be collected and transported to be viable for any application. The initial collection mechanism caused a pressure gradient at the output and depending upon the amount of material in the output orifice, the diameter would vary. This variation in the sample would cause the standard deviation to be too high rendering the sample unusable. The need for an output with a minimized pressure gradient was sought after and it was found that a wedge cut at the orifice of the device allowed for easier collection and did not alter the production of the sample based on the amount of material at the output.

Chapter 7

Conclusion

A microfluidic flow focusing device was able to create uniform sub-micron and micron-sized ADV agents. These agents were susceptible to ultrasound pressure for applications such as vessel occlusion, controlled drug delivery, and contrast enhancement. A pressure control flow system allowed for effortless tuning of droplet diameter and allowed for the first ever sub-micron ADV droplet creation with the use of microfluidics.

Chapter 8

Publications

- Precision Manufacture of Phase-Change Perfluorocarbon Droplets using Microfluidics (9.1)
- Published in Ultrasound in Medicine & Biology
  - Reproduced with permission from Elsevier.
  - Vol. 37, No. 11, pp. 1952-1957, 2011
  - Final form August 17th
- High-speed, clinical-scale microfluidic generation of stable phase-change droplets for gas embolotherapy (9.2)
  - Published in Lab on a Chip
    - Reproduced by permission of The Royal Society of Chemistry.
  - DOI: 10.1039/C1LC20615J
  - Accepted September 5th
- Microfluidic generation of acoustically active nanodroplets (9.3)
  - In preparation for submission to Small

8.1 Precision Manufacture of Phase-Change Perfluorocarbon Droplets using Microfluidics [1]

Thomas D. Martz[1], Paul S. Sheeran[2], David Bardin[3], Abraham P. Lee[3], and Paul A. Dayton[2],*

[1]Curriculum of Applied Sciences and Engineering - Materials Science, The University of North Carolina, Chapel Hill, NC, 27599

[2]Joint Department of Biomedical Engineering, The University of North Carolina and North Carolina State University, Chapel Hill, NC, 27599

[3]Department of Biomedical Engineering, The University of California at Irvine, Irvine, CA, 92697

8.1.1 Abstract

Liquid perfluorocarbon droplets have been of interest in the medical acoustics community for use as acoustically activated particles for tissue occlusion, imaging, and therapeutics. To date, methods to produce liquid perfluorocarbon droplets typically result in a polydisperse size distribution. Because the threshold of acoustic activation is a function of diameter, there would be benefit from a monodisperse population to preserve uniformity in acoustic activation parameters. Through the use of a microfluidic device with flow-focusing technology, the production of droplets of perfluoropentane with a uniform size distribution is demonstrated. Stability studies indicate that these droplets are stable in storage for at least two weeks. Acoustic studies illustrate the thresholds of vaporization as a function of droplet diameter, and a logarithmic relationship is observed between acoustic pressure and vaporization threshold within the size ranges studied. Droplets of uniform size have very little variability in acoustic vaporization threshold. Results indicate that microfluidic technology can enable greater manufacturing control of phase-change perfluorocarbons for acoustic droplet vaporization applications.

Keywords: Acoustic droplet vaporization, Ultrasound, Monodisperse, Perfluoropentane, Microfluidic

[1]

8.1.2 Introduction

Acoustic Droplet Vaporization Agents

In acoustic droplet vaporization (ADV), acoustic pressure delivered to a liquid droplet by an ultrasound (US) transducer provides the additional energy necessary to induce a liquid-to-gas phase transition. This phase transition allows for unique applications that are not possible with standard microbubble contrast agents, because ADV agents exhibit a very large volume change after activation. In addition, ADV agents are typically poorly echogenic in their liquid form, but highly echogenic as gas bubbles.

The basic construction of an ADV agent consists of a volatile liquid core that can be converted to a gas with additional energy. Typically, ADV droplets consist of perfluorocarbons (PFC) such as perfluoropentane (PFP) (Zhang et al., 2010), perfluorohexane (PFH) (Giesecke and Hynynen, 2003; Fabiilli et al., 2010b), or perfluorooctane (Fabiilli et al., 2009). The most commonly used PFCs, PFP and PFH, have boiling points near physiological temperatures (29°C and 56°C, respectively). Recently, stabilization and ADV capability of droplets of liquid perfluorobutane (boiling point of -1.7°C) has been demonstrated (Sheeran et al., 2011a).

Producing (PFC) droplets in the micron and sub-micron range increases the Laplace pressure exerted on the liquid core, enabling small droplets to be maintained in liquid form even above their vaporization temperature. The addition of a stabilizing shell reduces droplet coalescence and increases stability of the emulsions (Kripfgans et al., 2005; Rapoport et al., 2009b; Sheeran et al., 2011a). Commonly utilized methods of producing PFC droplets include sonication or high-speed mechanical agitation of the host solution, which typically results in a polydisperse population (Fabiilli et al., 2010b; Rapoport et al., 2010).

Acoustic Droplet Vaporization Applications

Liquid perfluorocarbon droplets have been shown to provide ultrasound image contrast (Kripfgans et al., 2002; Marsh et al., 2007), although the backscatter is notably less than similarly sized microbubble agents. One of the first commercial applications of perfluorocarbon droplets for US contrast enhancement was Echogen (Sonus Pharmaceuticals, Bothell, WA, USA), a perfluoropentane emulsion (Quay, 1998). Clinical trials for Echogen were abandoned in 2000 before FDA approval could be obtained.

Once vaporized, ADV agents are readily detectable by an imaging system even at low concentrations. In very small amounts, droplets when converted to bubbles through

ADV could act as point beacons for phase aberration corrections (Apfel, 1998; Haworth et al., 2008). The unique advantages of ADV droplets in the 100-nm size range is that they have the potential to extravasate from the vasculature and into the tissue, enabling ADV-based contrast imaging or therapy to extend beyond the vascular space, where traditional microbubbles cannot access (Rapoport et al., 2007; Rapoport et al., 2009a; Sheeran et al., 2011a).

One of the most well studied applications of ADV is embolotherapy. This technique enables the intentional creation of an occlusion in a specific tissue to limit blood flow. This has been proposed to treat renal cell carcinoma, to reduce blood loss for hypervascular tumors, and to treat hemorrhaging (Kripfgans et al., 2002; Zhang et al., 2010). Kripfgans et al. (2005) (Kripfgans et al., 2005) demonstrated that a filtered emulsion of droplets, which is intra-arterially injected, can reduce kidney perfusion by 70 %. This level of organ perfusion reduction has the ability to cause ischemic necrosis for therapeutic applications, or it can enhance the utility of radiofrequency tissue ablation by minimizing thermally dissipative effects due to reduced flow (Kripfgans et al., 2005). A second application of ADV agents is site-specific therapeutics, where the goal is to deliver a potent agent only to the disease site while minimizing systemic effects. The ADV-mediated delivery of a chemotherapeutic drug directly to the tumor has been shown to mediate regression of ovarian and breast cancer (Rapoport et al., 2009b). ADV agents that have the ability to carry a therapeutic payload to a desired vessel could be combined with vessel occlusion upon activation to allow for an increase in residence time of the therapeutic agent (Fabiilli et al., 2010b).

With spatial and temporal control over ADV agent activation, ADV agents can be used as a nucleation site for high-intensity focused ultrasound (HIFU) tumor ablation. During HIFU, the microdroplets can be activated to increase the therapeutic effect or decrease the treatment time (Zhang and Porter, 2010; Zhang et al., 2011).

Considerations of ADV agent size distribution

The size of ADV agents is an important factor in determining the vaporization threshold and the biodistribution. The Antoine equation predicts a negative logarithmic relation between droplet size and activation energy, where larger droplets require less energy to vaporize than smaller droplets (Rapoport et al., 2009a). Most who have characterized ADV-based agents have evaluated a polydisperse droplet population. Although general trends in thresholds have been observed, polydispersity in droplet sizes has led to a variability in the vaporization threshold measured for studies that examine a bulk population of ADV droplets. In addition, the larger droplets vaporize

at lower energies and the resulting bubbles can influence the threshold energy for the smaller droplets (Lo et al., 2007), confounding *in-vitro* characterization of vaporization thresholds. Because microbubbles combined with high acoustic pressures can lead to unwanted bioeffects (Miller et al., 2008), it may be desirable to perform ADV at the minimum acoustic pressure required. A polydisperse sample may require a higher pressure to efficiently vaporize the entire population due to smaller droplets requiring more energy.

For micron-sized ADV agents, one of the primary applications is vessel occlusion, where it may be important to have a well-characterized distribution of droplet sizes to target a specific vascular diameter while not affecting other vessels (Kripfgans et al., 2005). For the same reasons, a droplet designed for imaging applications that is too large could lodge in the lungs or other organs after IV injection, leading to undesired vessel occlusion. All of these limitations are motivating reasons for precise size control of ADV agents.

Previous studies to improve the size distribution characteristics of perfluorocarbon droplets have involved microfluidic sorting (Huh et al., 2007) and filtering (Kripfgans et al., 2005). The microfluidics platform is well known for the ability to create particles, droplets (Tan et al., 2004; Xu et al., 2006; Teh et al., 2008), microbubbles (Hettiarachchi et al., 2007a), and multi-layer particles (Hettiarachchi et al., 2009) of uniform size. In this manuscript, we assess the feasibility for producing a monodispersed ADV agent through a microfluidic technique to achieve uniform activation thresholds.

8.1.3 Materials and Methods

Reagent Preparation

Lipid PFP was purchased from FluoroMed, L.P. (Round Rock, Texas, USA). Lipid solutions were created using a 9:1 molar ratio of 1,2-distearoyl-sn-glycero-3-phosphocholine (DSPC) (Avanti Polar Lipids, Alabaster, AL, USA) and 1,2-distearoyl-sn-glycero-3-phosphoethanolamine-N[methoxy-(polyethylene glycol)-2000] (DSPE-PEG2000) (Avanti Polar Lipids) in a 110-mL solution of deionized (DI) water, glycerol (Fisher Scientific, Pittsburgh, PA, USA), propylene glycol (Fisher Scientific, Pittsburgh, PA, USA), and pluronic F-68 (Sigma-Aldrich Corporation , St. Louis, MO, USA).

Fifty mg of DPSC and 19.6 mg DSPE-PEG2000 were dissolved in chloroform. The chloroform was then evaporated with N2, after which 50 mL of DI water was added and the resulting solution was sonicated for 20 minutes. After sonication, 47 mL DI

water, 2 mL glycerol, 1 mL propylene glycol, and 10 mL pluronic F-68 were added. The solution was vortex mixed for 1 minute and then sonicated for 10 minutes.

Microfluidic Device Fabrication

The process for developing the microfluidic wafer has been previously described by Hettiarachchi el al. (2009) (Hettiarachchi et al., 2009). Briefly, the channels were created using Illustrator (Adobe, San Jose, CA, USA) and printed (20,000 dpi) by CAD/Art Services (Brandon, OR, USA). In a clean room, the wafer was first oxidized in oxygen plasma and then spin-coated with a UV curable epoxy (SU-8-25, MicroChem, Newton, MA, USA). On exposing the wafer to UV light, the channel patterns develop to use as a negative for device production.

With the wafer in a petri dish, Polydimethylsiloxane (PDMS) (Dow Corning, Midland, MI, USA) and a curing agent were poured over the wafer at a 10:1 ratio, respectively. This was then placed under vacuum for 24 h and then cured at 60°C overnight. After the PDMS was cured, the individual microfluidic devices were removed from the wafer. The individual microfluidic device and a clean microscope slide (2947-75X25, Corning, Corning, NY, USA) were placed in a plasma cleaner (Harrick Plasma, Ithaca, NY, USA) and exposed to a plasma field under a controlled pressure of 500 mTorr for 3 minutes. Upon completion of the plasma cleaning process, the PDMS and glass slide were immediately joined, forming complete microchannels. One minute after the bond was established, DI water was injected into the channels to create a hydrophilic environment.

Microfluidic Experimental Apparatus

The microfluidic experimental apparatus was set up similar to that as described previously by Kaya et al. (2010)(Kaya et al., 2010). Briefly, the microfluidic device was secured to a moving stand on an inverted microscope (Olympus 1X71 microscope, Center Valley, PA, USA), and viewed with a 50X NA = 0.5 objective. A high speed camera (Fastcam APX-RS, Photron, Inc., San Diego, CA, USA) was used to capture images and videos of the device output. Reagents were injected from syringes into device channels through Tygon S-54-HL tubing (Saint-Gobain Performance Plastics, Akron, OH, USA). Calibrated syringe pumps (Harvard Apparatus, Holliston, MA, USA) were used to control rate of material flow in individual microchannels.

Sample Production

To produce uniform samples, the PFP flow rate was fixed at a constant value and the lipid flow rate was increased until the smallest stable droplets were formed. The system was allowed to stabilize for 5 minutes before collection, because pressure changes

in the system required a few minutes to equalize. This process was repeated across a range of different flow rates, as described in Table 8.1. To determine the production rate for the microfluidic device, high-speed video analysis of the droplet production was performed. Time stamps enabled the determination of droplet production rate.

Acoustic Experimental Apparatus

The experimental setup to determine droplet vaporization thresholds was similar to that previously described by Sheeran et al. (2011)(Sheeran et al., 2011a). Briefly, a heated water bath maintained at 37°C was connected to an inverted microscope. Droplets were injected through a nearly acoustically and optically transparent microcellulose capillary tube with an inner diameter of 200 µm (Spectrum Labs, Inc., Greensboro, NC, UNC). A 5-MHz piston transducer (IL0506HP, Valpey Fisher Corp., Hopkinton, MA, USA) was positioned in the water bath confocally with a water immersion microscope objective (100x, NA=1.0). The output of the ultrasound transducer was calibrated by inserting a needle-hydrophone (HNA-0400, Onda Corp., Sunnyvale, CA, USA) into the experimental system at the exact location where the samples are positioned during activation studies (the focus of the microscope objective). Droplets were exposed to single 10-cycle sinusoidal pulses while the ultrasound pressure was increased incrementally until droplet vaporization was observed. The procedure was repeated for at least 20 droplets from each size distribution to verify droplet size and threshold.

Stability Analysis

Droplets were stored at 4°C in 3-mL vials until sampling. For analysis, a 25-µliter aliquot of droplets was placed on a glass slide, and images were captured with the Photron Fastcam camera. Size measurements were performed in ImageJ (NIH, Bethesda, MD, USA) by comparison to a calibrated reticle (Edmund Industrial Optics, Barrington, NJ, USA). A minimum of 50 droplets was measured for each population.

8.1.4 Results

The dimensions of the microfluidic device, material composition, and flow rates all have the ability to alter the composition of the resulting droplet. Due to the microfabrication process, there are minute variations from device to device (we measured a 13% deviation in orifice widths across 10 devices). With this in mind, only one device was used for the duration of production to ensure that the dimensions of the device were unchanged. The material compositions also went unchanged to ensure that the

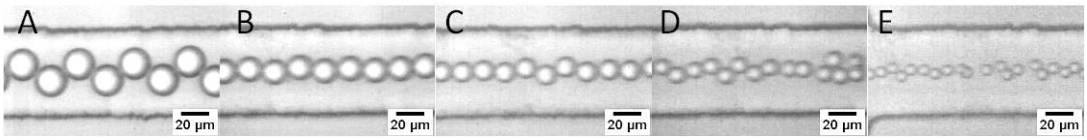

Figure 8.1: High-speed video frames of microfluidic droplet production at diameters of (a) 20.4±0.3 µm, (b) 16.2±0.5 µm, (c) 12.6±0.5 µm, (d) 10.3±0.4 µm and (e) 7.4±0.4 µm, corresponding to lipid and PFP flow rates of lipid 40 µL/min; PFP 12.5 µL/min, lipid 31 µL/min; PFP 15 µL/min, lipid 40 µL/min; PFP 15 µL/min, lipid 50 µL/min; PFP 15 µL/min, lipid 60 µL/min; and PFP 13.9 µL/min, respectively.

droplets would experience a standardized reaction to the US pressure.

Precision Size Control

The flow rates were varied over five sets of conditions for the duration of the experiment to alter the droplet diameter. Results illustrated that by varying flw rates, the PFP population diameters could be carefully selected. In general, as the lipid flow rate was increased, droplet size decreased (Figure 8.1). As the PFP flow rate was increased, droplet size increased. Table 2 lists the flow rates, mean droplet size, standard deviation, and polydispersity index (Xu et al., 2006).

For the populations studied, the standard deviation was largest for the smallest droplets (SD=0.4 for the 7.4 micron population) and smallest for the largest droplets (0.3 for the 20.4 micron population). All populations had a polydispersity index of 5.1 or less.

Production Rate

The 20-µL/min lipid and the 12.5-µL/min PFP flow rates, which resulted in 20.4 micron droplets, had a production rate of 1.85×10^4 droplets produced per second (slowest production sample); whereas the 60-µL/min lipid and 13.9-µL/min PFP flows, which produced 7.4 micron droplets, had a production rate of 1.65×10^5 droplets per second (fastest production sample). Table 3 lists the production rates for the 5 samples.

Acoustic Responses

The five samples were diluted and injected into a cellulose microcapillary tube where droplets from each population were individually subjected to US. The US data showed that there was a distinct vaporization threshold pressure for each diameter (Figure 8.2).

Creation Data				
Lipid (μL/min)	PFP (μL/min)	Average (μm)	Standard Deviation	Polydispersity
20	12.5	20.4	0.3	1.5
31	15	16.2	0.5	3.4
40	15	12.6	0.5	3.9
50	15	10.3	0.4	3.5
60	13.9	7.4	0.4	5.1
3 Day Data				
20	12.5	20.6	0.5	2.6
31	15	16.2	0.4	2.6
40	15	12.6	0.4	3.4
50	15	10.5	0.4	3.9
60	13.9	7.5	0.5	6.2
1 Week Data				
20	12.5	20.4	0.5	2.6
31	15	15.5	0.4	2.8
40	15	12.6	0.4	3.1
50	15	10.7	0.4	3.4
60	13.9	7.5	0.4	4.7
2 Week Data				
20	12.5	20.4	0.5	2.7
31	15	15.5	0.5	3.4
40	15	12.2	0.4	3.2
50	15	10.8	0.4	3.5
60	13.9	7.5	0.7	9.0

Table 8.1: Polydispersity data for the five studied droplet populations from the day the droplets were created and at three days, one week and two weeks.

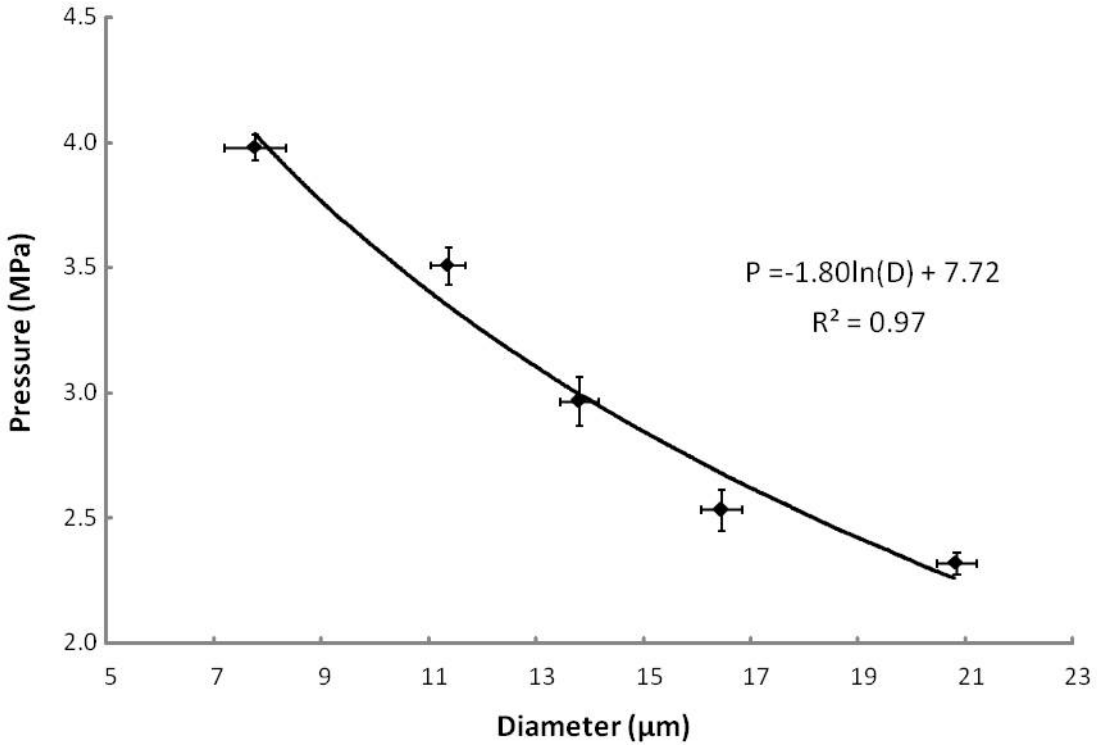

Figure 8.2: Average pressure of vaporization *vs.* average droplet diameter. Error bars indicate standard deviations in pressure and diameter. The trendline is logarithmic.

The data trend suggests a logarithmic relationship (P = -1.80ln(D) + 7.72, $R^2 = 0.97$), as predicted by the Antoine equation.

Long-tem stability

Populations maintained a fairly low polydispersity over a two week time period (Table 2), and overall, the mean diameters of the populations drifted less than 4.6% (Figure 8.3). The 16.2- and 10.3-µm mean diameter populations each maintained the same polydispersity, and the 20.4-, 12.6- and 7.4-µm mean diameter populations changed by a factor of 1.8, 1.3, and 1.9, respectively.

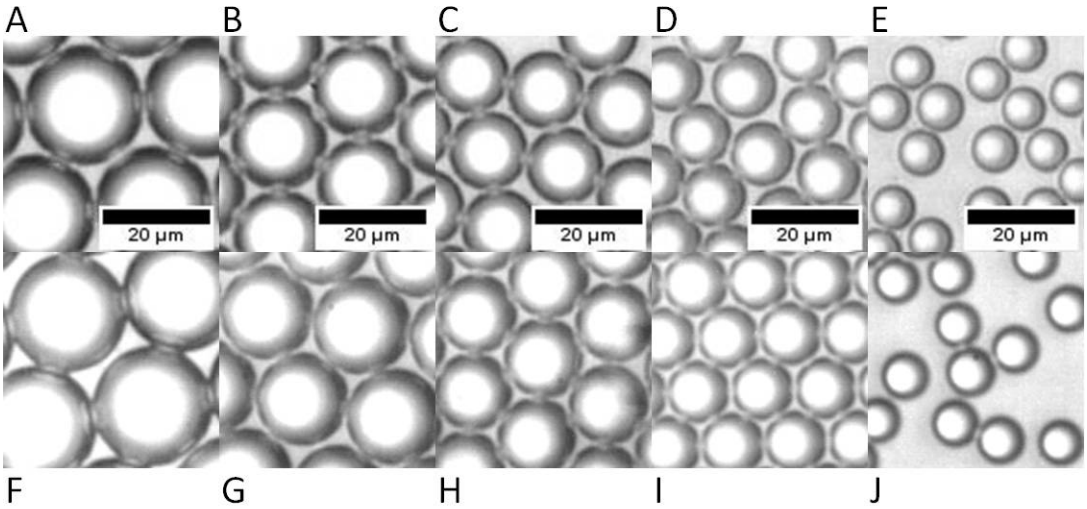

Figure 8.3: Microscopy images of droplets one week apart illustrating size stability. (a–e) One week after production— populations of mean diameter of (a) 20.4±0.3 µm, (b) 16.2±0.5 µm, (c) 12.6±0.5 µm, (d) 10.3±0.4 µm and (e) 7.4±0.4 µm. (f–j) Two weeks after production—populations corresponding to (a–e), respectively, with mean diameters of (f) 20.4±0.5 µm, (g) 15.5±0.5 µm, (h) 12.2±0.4 µm, (i) 10.8±0.4 µm and (j) 7.5±0.7 µm.

Lipid (µL/min)	PFP (µL/min)	Production Rate (Droplets/sec)
20	12.5	1.85×10^4
31	15	3.31×10^4
40	15	6.44×10^4
50	15	1.03×10^5
60	13.9	1.65×10^5

Table 8.2: Production rates for droplets produced with microfluidics under varying input flow conditions.

8.1.5 Discussion

The method described here demonstrates the potential of production of uniform-sized droplets for acoustic droplet vaporization using microfluidics. Data illustrate that this technique enabled production of a population of droplets where each droplet responded similarly to the same acoustic parameters because of uniform size. One advantage of utilizing such uniform droplets would include the ability to use the lowest acoustic pressure possible for vaporization (because all droplets would respond similarly), thereby achieving the highest vaporization efficiency for the lowest acoustic pressure. Keeping the acoustic pressure as low as required would conform to the "As Low As Reasonably Achievable (ALARA) Principle" for clinical ultrasonics. Other potential advantages of uniform sized ADV agent production, although not demonstrated here, would be the ability to tailor droplet sizes for specific vessel occlusion, or to enable precision drug-loading for therapeutic-carrying ADV agents.

Microfluidic techniques have previously demonstrated unique utility in the controlled fabrication of droplets and microbubbles. The biggest limitation to this method to date is that the production rate is substantially slower than other droplet and microbubble production methods. Even for the fastest production method here, it would require nearly 3 h to achieve $1x10^9$ droplets (a similar order of magnitude to the concentration of microbubble contrast agents prepared by a mechanical agitation method). However, in the future microfluidic techniques may be scaled up to achieve higher throughput, although the need to maintain identical dimensions and flow rates to each orifice in order to preserve size uniformity presents a challenge. It should also be noted that although the smallest droplets described here were approximately 7 microns, which is likely too large for *in vivo* application, this size was limited only by our particular system, and is not a fundamental limit of microfluidic droplet production. It is very reasonable to anticipate that by optimizing the channel dimensions, component flow rates, and the lipid/perfluorocarbon ratios, that droplets much smaller than 7 microns can be prepared. Prior studies have illustrated microfluidic production of liquid droplets as small as 100 nanometers (Tan and Lee, 2005).

8.1.6 Conclusion

A microfluidic device can produce monodisperse PFP/lipid droplets using flow focusing technology. Monodispersed PFP/lipid droplets that were subjected to US pressure waves showed a uniform ADV response. The relationship formed by droplet diam-

eter and ADV threshold agreed with the expected negative logarithmic response based on the size of the droplets. Droplet populations produced with microfluidics were stable within the two-week time period studied.

8.1.7 Acknowledgements

The authors would like to thank Jason Streeter for the preparation of the lipid solution and Roger Shih for the microfluidic wafer fabrication. Also, the authors appreciate the assistance from Dennis Given and Roshni Kothadia for their work in droplet characterization and data organization. This project was supported by R01EB008733 and R21EB011704.

8.2 High-speed, clinical-scale microfluidic generation of stable phase-change droplets for gas embolotherapy [2]

David Bardin,[a] Thomas D. Martz,[b] Paul S. Sheeran,[c] Roger Shih,a Paul A. Dayton[c] and Abraham P. Lee*[a]

[a]Department of Biomedical Engineering, University of California, 3406 Engineering Hall, Irvine, CA, 92697, USA

[b]Curriculum of Applied Sciences and Engineering—Materials Science, The University of North Carolina, Chapel Hill, NC, 27599, USA

[c]Joint Department of Biomedical Engineering, The University of North Carolina and North Carolina State University, Chapel Hill, NC, 27599, USA

8.2.1 Abstract

In this study we report on a microfluidic device and droplet formation regime capable of generating clinical-scale quantities of droplet emulsions suitable in size and functionality for *in vivo* therapeutics. By increasing the capillary number—based on the flow rate of the continuous outer phase—in our flow-focusing device, we examine three modes of droplet breakup: geometry-controlled, dripping, and jetting. Operation of our device in the dripping regime results in the generation of highly monodisperse liquid perfluoropentane droplets in the appropriate 3–6 µm range at rates exceeding 10^5 droplets per second. Based on experimental results relating droplet diameter and the ratio of the continuous and dispersed phase flow rates, we derive a power series equation, valid in the dripping regime, to predict droplet size, $D_d \cong 27(Q_C/QD)^{-5/12}$. The volatile droplets in this study are stable for weeks at room temperature yet undergo rapid liquid-to-gas phase transition, and volume expansion, above a uniform thermal activation threshold. The opportunity exists to potentiate locoregional cancer therapies such as thermal ablation and percutaneous ethanol injection using thermal or acoustic vaporization of these monodisperse phase-change droplets to intentionally occlude the vessels of a cancer.

8.2.2 Introduction

Embolization has emerged as an accepted modality for the treatment of various cancers, including hepatocellular carcinomas, hepatic metastases, and renal cell carcinomas.(Goode and Matson, 2004) The intentional occlusion of a vessel, embolization enables the reduction of blood flow into or out of that vessel, and has typically been used in cancer therapies to produce local ischemia resulting in tumor necrosis. Established methods of embolization include the placement of a metal coil or soluble gelatin sponge within the target blood vessel, or the injection of chemical or particulate agents such as ethanol or polyvinyl alcohol particles to reduce blood flow at the site of injection or immediately downstream.(Goode and Matson, 2004; Kalman and Varenhorst, 1999)

Recently the field of medical ultrasound has shown much interest in gas embolotherapy, in which acoustic or thermal energy induces a droplet emulsion with a volatile liquid core to undergo a liquid-to-gas phase transition, and volume expansion, to strategically form gas emboli *in vivo*, as shown in Fig. 8.4. Acoustic droplet vaporization (ADV) specifically refers to the use of focused ultrasound to induce such a transition, in which the applied acoustic pressure supplies the necessary energy to induce superheated droplet emulsions to vaporize into microbubbles. The phase-change typically results in microbubbles five to six times larger in diameter than the original droplets, enabling these gas bubbles to occlude vessels of sufficiently small diameters, such as capillaries and some arterioles.(Apfel, 1998; Kripfgans et al., 2000)

Studies thus far have investigated the usefulness of ADV agents to enhance contrast in ultrasound imaging,(Kripfgans et al., 2002) to deliver therapeutics,(Rapoport et al., 2010; Fabiilli et al., 2010a; Fabiilli et al., 2010b) for enhanced thermal delivery alongside highintensity focused ultrasound (HIFU),(Zhang and Porter, 2010) and for occlusion in animal models.(Zhang et al., 2010) The choice of liquid core consists of a number of perfluorocarbons, including perfluoropentane,(Kripfgans et al., 2000; Fabiilli et al., 2010b; Fabiilli et al., 2010a; Zhang et al., 2010; Kripfgans et al., 2004; Lo et al., 2007; Rapoport et al., 2009b; Giesecke and Hynynen, 2003; Schad and Hynynen, 2010) perfluorohexane, (Fabiilli et al., 2010b; Giesecke and Hynynen, 2003) perfluorooctane,(Fabiilli et al., 2009) and perfluorobutane.(Sheeran et al., 2011a) Encapsulation of the liquid core inside a lipid, albumin or polymer shell reduces coalescence among

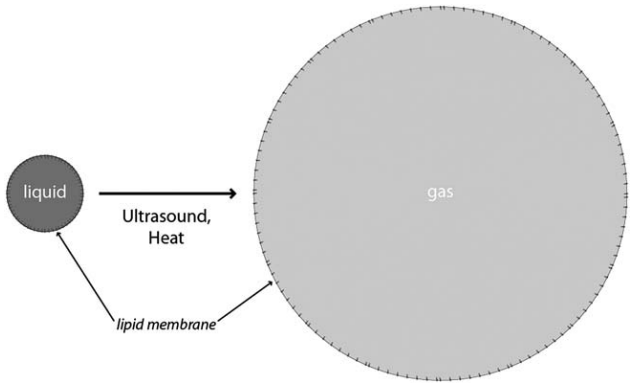

Figure 8.4: Schematic of the liquid-to-gas phase transition of a phase-change droplet. When presented with acoustic or thermal stimuli of a threshold amount, the volatile liquid core of the droplet rapidly vaporizes within the lipid shell. Expansion to a gas bubble enables the intentional occlusion of a target vessel *in vivo*. Other possible stimuli include light and mechanical pressure.

the droplet population and increases the Laplace pressure sufficiently to enable these volatile emulsions to remain as superheated droplets at body temperature.(Kripfgans et al., 2000; Giesecke and Hynynen, 2003)

Current methods to generate these phase-change droplets— which include sonication and high-speed mechanical agitation— typically result in a polydisperse size distribution(Rapoport et al., 2010; Fabiilli et al., 2010a) and a nonuniform acoustic activation threshold, as well as droplets either too large for passage through the lung capillaries (>6 µm) or too small to occlude the desired vessel (<1 µm).(Kripfgans et al., 2000; Zhang et al., 2010) Thus required are secondary methods of size selection such as filtering(Kripfgans et al., 2002; Lo et al., 2006) or microfluidic sorting(Huh et al., 2007) to control the sizes of these distributions. The Antoine equation predicts a negative logarithmic relationship between vaporization energy and droplet diameter,(Rapoport et al., 2009b) meaning that small droplets require more energy to vaporize than larger droplets due to increased Laplace pressure. Hence, narrowing the droplet size distribution such that it is highly monodisperse should result in a uniform response to focused acoustic pressure. As well, a monodisperse population of ADV agents may better target a specific vessel diameter to improve occlusion efficiency and efficacy, and would significantly reduce unwanted bioeffects seen *in vivo*, including delayed febrile-like reactions and respiratory distress.(Zhang et al., 2010; Kripfgans et al., 2000)

Droplet-based microfluidic systems have shown to be effective technologies to produce droplets(Tan et al., 2004; Nisisako et al., 2002) and microbubbles(Hettiarachchi

et al., 2007b; Talu et al., 2007; Talu et al., 2008) in the micrometre diameter range with high uniformity. Yet despite the attractiveness of precision control over size, shape, and composition, these systems have traditionally been viewed as unviable as bulk manufacturing processes owing to relatively low generation rates. At present, reporting of clinical-scale generation of droplet or microbubble emulsions has been limited, and virtually absent for emulsions truly useful for *in vivo* intravenous or intra-arterial therapeutics. Most recently Castro-Hernandez et al.(Castro-Hernandez et al., 2011) described a new regime for microbubble generation dependent on the formation of a strong pressure gradient at the bubbleproducing region. Approximately 5 µm in diameter gas-in-water bubbles were successfully generated at the tip of a long gas ligament with rates exceeding 10^5 Hz from a single channel, though bubbles were unstable due to the lack of significant surfactant or lipid shells. Far less impressive per-channel frequencies have been observed in liquid–liquid droplet generation systems. Nisisako and Torii(Nisisako and Torii, 2008) achieved a throughput of 320 mL h^{-1} in generating approximately 100 µm droplets using a multilayer device with 256 droplet formation units and a breakup rate of $1.4x10^3$ droplets per second per cross-junction. Kobayashi et al.(Kobayashi et al., 2007) reported the formulation of oil-in-water emulsions at cumulative rates up to $2.2x10^4$ Hz using a total of 1500 submicron-channels on single-crystal silicon plates, although the emulsions were only moderately monodisperse with a minimum coefficient of variation (CV) of 9%. In fact, frequency distributions for various liquid–liquid droplet generation systems, whether water in oil or oil in water, rarely exceed several thousand droplets per second from a single channel in forming droplets seldom smaller than 10 µm in diameter.(Teh et al., 2008) From a healthcare perspective, one could comment that there is no practical use for these aforementioned emulsions due to either insufficient quantity or inappropriate characteristics of the emulsion. Thus, a need in microfluidics still exists for systems capable of generating clinical-scale amounts of droplet or microbubble emulsions with suitable size and functionality for therapeutics.

To overcome the limitations of past droplet generation systems, we considered the basic mechanisms of droplet generation with the intent to find a possible route to produce, in mass, micrometre-scale droplets with engineered biology. Recent publications on the physics of fluids have reported the observation of a number of distinct droplet formation modes in flowfocusing microfluidic devices.(Anna and Mayer, 2006; Cubaud and Mason, 2008) Under controlled experimental conditions, such a device transitions from geometry-controlled mode to dripping to jetting, affecting the size and generation frequency by up to an order of magnitude. In particular, Anna and Mayer(Anna

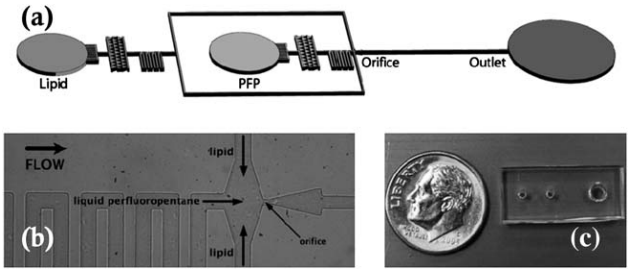

Figure 8.5: Geometry of the device for the generation of liquid perfluoropentane phase-change droplets. (a) Schematic view of the microfluidic flow-focusing device. All channels are rectangular with a height of 25 µm. (b) Image of the flow-focusing region. Lipid solution and liquid perfluoropentane distribution channels measure 38 µm in width and direct flows to a 7 µm orifice. Expanding nozzle geometry precedes a postorifice channel 30 µm in width. (c) Overhead view of the assembled PDMS device relative to a dime.

and Mayer, 2006) allude to the dripping mode of droplet breakup as a method to yield droplets smaller than the minimum device feature size with a shorter primary breakup period than other modes, as yet demonstrated in the literature with a healthcare intent. We thus set out to use the dripping regime to meet our objective of the clinic-ready manufacture of liquid perfluoropentane droplets as phase-change agents for cancer treatment.

In this work we present a microfluidic device, operated in the dripping regime, for the super high-speed generation ($>10^5$ Hz) of monodisperse liquid perfluoropentane droplets in the desired size range for gas embolotherapy. Resulting droplet populations exhibit polydispersity index values of $<5\%$, are stable at room temperature for several weeks, and are thermally vaporized at 88°C in a water bath. These liquid perfluoropentane droplets thus exhibit phase-change and are ideal for targeted vessel occlusion alongside such cancer therapies as HIFU, radiofrequency ablation (RFA), laser ablation (LA), laser-induced thermotherapy (LITT), and chemotherapy. Our microfluidic device, shown in Fig. 8.5, features a hydrodynamic flow-focusing region and expanding nozzle geometry to generate monodisperse liquid perfluoropentane droplets encapsulated in a lipid shell.

8.2.3 Materials and methods

Device design

The microfluidic device, made of polydimethylsiloxane (PDMS) on a glass substrate, consists of fixed geometric channels designed to direct liquid perfluoropentane and a lipid solution to an orifice 7 µm in width. Filter channels of the same dimension immediately follow both inlets to prevent clogging at the orifice. Serpentine distribution channels increase the resistance between inlets and the orifice chamber, minimizing the susceptibility of droplet generation to disruptions in the fluid flows and increasing the pressure drop along the longitudinal axis of the device. Liquid perfluoropentane and lipid distribution channels each measure 38 µm in width. The post-orifice channel measures 30 µm in width.

Device operation: droplet formation regimes

The principle behind a microfluidic flow-focusing system is to force a central stream of a dispersed phase and two side sheath flows of a continuous phase through a small orifice, causing a focusing effect and a breaking of the thread at the orifice into uniform emulsions.(Tan et al., 2006)

Most traditional flow-focusing devices have been operated in the geometry-controlled mode, termed for the large dependence of droplet size on the smallest feature size in the device—the orifice. In this mode droplets break off from the dispersed phase finger following a protrude-and-retract mechanism.(Garstecki et al., 2005) Droplets in the geometry-controlled mode are highly monodisperse but limited in minimum size by the width of the orifice.

An increase in the capillary number $\mathrm{Ca} = \eta \mathrm{V}/\gamma_{EQ}$, where η is the viscosity, V is the superficial velocity of the continuous outer phase, and γ_{EQ} is the equilibrium surface tension between the two fluid phases, leads to droplet generation in the dripping regime.(Anna and Mayer, 2006) This regime produces monodisperse droplets smaller than the size of the orifice due to narrowing of the dispersed phase finger. The dripping mode is characterized by a dispersed phase tip that does not retract but rather remains at a fixed location in the orifice, generating a stream of droplets off the tip due to Rayleigh capillary instability.

A further increase in the capillary number leads to droplet generation in the jetting mode, wherein the dispersed phase finger extends far into the post-orifice channel. Droplets, which break off the tip of the dispersed phase finger due again to Rayleigh capillary instability, tend to be as large as or larger than the orifice width in the jetting mode and may be polydisperse.(Anna and Mayer, 2006)

By adjusting the flow parameters and continuous phase viscosity, we thus aimed to operate our flow-focusing microfluidic device in the dripping regime to attain droplets

of the desired size for gas embolotherapy (1–6 µm in diameter).

Microfabrication and assembly

Standard soft lithography techniques(Xia and Whitesides, 1998) were used to fabricate the microfluidic devices. Devices were designed as vector-based fluidic channel geometries in Illustrator (Adobe) and printed at 20 000 DPI by CAD/Art Services. In a class 10,000 clean room, a 25 µm layer of a UV-curable epoxy (SU8-25, MicroChem) was spun onto a 3 inch silicon wafer and exposed to UV-light through the photomask and developed.

Next, PDMS (Sylgard 184, Dow Corning), consisting of 10 : 1 prepolymer to curing agent, was poured over the patterned silicon wafer in a Petri dish to mold a silicon elastomer replica. The Petri dish was then vacuumed for at least half an hour to degas the PDMS and left overnight in a 70°C temperaturecontrolled dry oven to cure fully. The device was peeled from the hard master in a laminar flow chamber and inlets and outlet were punched using a blunt 18G needle. A soda lime glass slide was cleaned with isopropyl alcohol prior to use as the substrate. The cured PDMS device and clean glass slide were bonded after 150 seconds in air plasma at 250 milliTorr. DI water was added to the outlet after plasma preparation and allowed to wick in order to maintain the hydrophilicity of the channels.

Chemicals

A lipid shell was chosen over an albumin shell, as albumin shells have shown an increased tendency to become lodged in the pulmonary capillaries.(Zhang et al., 2010) Adapted from Hettiarachchi et al.,(Hettiarachchi et al., 2009) the lipid flow stream consists of an aqueous glycerol mixture with the stabilizing lipids DSPC (1,2-distearoyl-sn-glycero-2-phosphocholine, Avanti Polar Lipids) and DSPE-PEG2000 (1,2-distearoyl-sn-glycero-3-phosphoethanolamine-N-[methoxy(polyethylene glycol)-2000], Avanti Polar Lipids). Briefly, 5 mg DSPC and 1.96 mg DSPE-PEG2000 were combined in a glass vial and dissolved in chloroform ($CHCl_3$, Sigma) to form a homogeneous mixture. The solvent was evaporated with a nitrogen stream and the vial was placed in a vacuum chamber for half an hour to ensure a complete dry. Five microlitres of ultra-pure water was added to the dry lipid mixture and sonicated at room temperature for 20 minutes. The solution was combined with an additional 1 mL of ultra-pure water, 4 mL of glycerol (Sigma), and 1 mL of nonionic surfactant (Pluronic F-68, Sigma), sonicated at room temperature for 10 minutes, and stirred overnight to ensure air saturation. The lipid solution was sonicated again for 15 minutes immediately prior to use to minimize unwanted liposome formation.

Perfluoropentane (dodecafluoropentane, C_5F_{12}, FluoroMed) was chosen as the liquid perfluorocarbon. Typical physical characteristics of perfluoropentane include a boiling point of 29°C—below the body temperature, 37°C—and a molecular weight of 288 g gmole^{-1}.

Imaging and characterization

The microfluidic device was mounted on an inverted microscope (IX71, Olympus) and external fluidic connections were made. The continuous lipid phase was supplied to the device via flexible tubing (Tygon, Sigma) and pumped at a volumetric flow rate of Q_L using a digitally controlled syringe pump (Pico Plus, Harvard Apparatus). The dispersed liquid perfluoropentane phase was delivered into the inlet of the microfluidic chamber using a homemade pressure pumping system controlled by an analytic regulator. Pressure pumping of the dispersed phase effectively minimized fluctuations in the liquid perfluoropentane flow and eliminated the buildup of pressure, characteristic of constant flow rate mechanical pumping, in the inner phase channels. Also, loading the liquid perfluoropentane was made easier by the homemade pressure pump as the low kinematic viscosity of this perfluorocarbon at room temperature (0.4 cSt) tends to complicate the loading of the syringe for mechanical pumping. The volumetric flow rate (µL min^{-1}) of the dispersed liquid perfluoropentane phase was determined from the droplet diameter D and the droplet generation frequency f_d as $Q_P = (\pi D^3/6)\ f_d$ x C, where C represents the necessary conversion factors. The 30-PSI limit of the analytical regulator prevented the use of pressure pumping for the continuous lipid phase.

A high-speed camera (V310 Phantom, Vision Research, New Jersey) was used to record videos of the droplet generation. The image analysis program ImageJ (NIH) was used for data processing and measurements. Production rates (droplets per second) were calculated from the videos by counting the number of droplets per 500 frames and multiplying by the frame rate. Droplet diameters were back calculated from area measurements of at least 50 droplets taken optically from recorded images using ImageJ. The polydispersity index $\sigma = \delta/D$ x 100% for each flow condition was calculated from the average droplet diameter D and standard deviation δ.

Droplet stability

Droplets were collected in the outlet well of the microfluidic device and transferred to a sealed 7 mL glass vial. In contrast to previous reports, which stored droplets at 4–5°C,(Zhang et al., 2010; Schad and Hynynen, 2010) droplets in this study were stored at room temperature to assess the viability of the droplets in an on-the-shelf setting. At Days 0 and 14, 300 µL aliquots of the droplet solution were pipetted onto glass

slides for stability studies. ImageJ was used to analyze at least 1000 droplets, imaged in population at 40x magnification, to establish average diameter and monodispersity over the two-week period.

Vaporization of droplets in a water bath

To determine the vaporization temperature of the perfluoropentane droplets, 300 µL aliquots of the droplet solution were added to 2 mL of dilute lipid solution in a 7 mL vented glass vial. The elevated density of liquid perfluoropentane (1.66 g mL^{-1}) relative to the solution meant that the droplets rested at the base of the vial. The vial was suspended in a stirred water bath and the bath temperature was gradually raised until we observed gas bubble formation and thus phase transition. The experiment was conducted twice again with pure liquid perfluoropentane and pure lipid solution as controls against unintended microbubble formation.

8.2.4 Results and discussion

Design optimization

Channel geometry, in addition to the compositions of fluid layers and the presence of surfactants, affects the stability of droplets post-production in the microfluidic device. Geometric optimization of the flow-focusing region enabled droplets to be produced in a single file, even at rates exceeding 10^5 Hz. To increase the distance between generated droplets at higher lipid and liquid perfluoropentane flow rates, the expanding nozzle and post-orifice channels were narrowed to widths of 70 µm and 30 µm. This narrowing minimized contact inhibitions in the highflow velocity environment of the expansion chamber, where shell resistances are low, preventing droplet fusion before collection in the outlet well.

Droplet formation regimes

By adjusting the flow parameters in our flow-focusing device, we observed each of the three distinct droplet formation regimes detailed. At low continuous phase flow rates Q_L, and correspondingly low dispersed phase pressures P_P, our device produced droplets in the geometry-controlled mode. As shown in Fig. 8.6a—comprising a series of overlaid images, successive in time—the dispersed phase finger, initially upstream of the orifice in this mode, protrudes beyond the constriction of the orifice and experiences a pinching from the sidewalls, causing droplets to shear off. This protrude-and-retract mechanism limits the droplet diameter to the width of the orifice. Droplets generated in the geometry-controlled mode ranged in diameter from 7.9±0.1 µm at 2.44x10^4 Hz

to 10.8±0.2 µm at 3.28x10^4 Hz.

Increasing the continuous phase flow (and, correspondingly, the capillary number) causes an abrupt transition to the dripping regime of droplet formation, characterized by a dispersed phase finger that narrows to a fine tip and remains in the orifice (Fig. 8.6b). Droplets, which break off the tip at high frequency due to ''steady'' Rayleigh capillary instability, vary in size according to the width of the dispersed phase finger rather than that of the orifice. Diameters of droplets generated in the dripping regime ranged from 3.6±0.2 µm at 1.36x10^5 Hz to 10.8±0.1 µm at 5.00x10^4 Hz.

High continuous phase flows paired with correspondingly high dispersed phase pressures transitioned droplet formation into the jetting mode. Fig. 8.6c overlays a series of images, successive in time, to demonstrate the break off of droplets in this mode due to ''dynamic'' Rayleigh capillary instability; relative to the dripping regime, the dispersed phase tip extends far beyond the orifice and fluctuates in both length and width. Droplets at the transition to the jetting regime ranged in diameter from 9.3±0.2 µm at 7.68x10^4 Hz to 13.5±0.1 µm at 3.84x10^4 Hz.

Generation of liquid perfluoropentane droplets

The flow rate parameters are determinants for stable production and precise control over the size and generation frequency of the liquid perfluoropentane droplets. In general and regardless of the droplet formation regime, the droplet diameter D—and consequently volume V—increases with the dispersed phase pressure P_P for a fixed continuous phase flow Q_L, consistent with previous studies.(Hettiarachchi et al., 2007b; Castro-Hernandez et al., 2011; Hettiarachchi et al., 2009) Shown in Fig. 8.7a, the width of the orifice limits the minimum droplet size in the geometry-controlled mode, while much smaller droplets can be generated in the dripping regime. The minimum droplet diameter tends to decrease with increasing Q_L, and thus increasing the capillary number, as the smallest droplets observed in this study occurred at the highest continuous flow rates.

An interesting observation emerged when establishing trends in the droplet generation frequency f_d (Fig. 8.7b). In geometrycontrolled mode, f_d tends to increase with P_P for a fixed Q_L in order to conserve mass. Conversely, for a given Q_L in the dripping regime, decreasing P_P significantly quickens the generation frequency (increases f_d) while reducing D, hence achieving the desired super high-speed generation of functional droplets suitable for therapeutic applications. Overall and as expected, f_d tends to increase with Q_L.

The sequence of high-speed images in Fig. 8.8 illustrates the general trends ob-

served in the dripping regime. In particular as droplets become small, the width of the dispersed phase finger heavily influences the diameter of the droplet after it breaks off from the tip.

Shown in Fig. 8.9 are droplet generation frequencies obtained from high-speed videos of production and corresponding polydispersity indexes, plotted as a function of droplet diameter. When operated in the dripping regime our device clearly produces liquid perfluoropentane droplets in the desired 3–6 µm range with high monodispersity at rates equal to or exceeding 10^5 Hz. Whereas no general trend appears to connect the droplet diameter and generation frequency in geometry-controlled mode, D tends to decrease as f_d quickens in the dripping regime. Simple adjustment of the flow parameters enabled the generation of droplets spanning a wide range of diameters, with a polydispersity index less than 5% for each condition.

Determining the liquid perfluoropentane volumetric flow rate Q_P as detailed, we evaluated the influence of the dimensionless flow rate ratio $\varphi = Q_L/Q_P$ on the droplet diameter and generation frequency. As shown in Fig. 8.10a, a key relationship emerges in the dripping regime relating D and φ to predict the droplet diameter based solely on the dimensionless flow rate ratio as: $D = 27.445\varphi^{-0.414}$ (r^2=0.99). Rounding, we characterize our flowfocusing droplet generator, operated in the dripping regime, in generic terms by

$$D_d \cong 27(Q_C/Q_D)^{-5/12}$$

where D_d represents the droplet diameter, and Q_C and Q_D represent the continuous and dispersed phase flow rates. Note that the exponent 5/12 matches the exponent reported by Castro- Hernandez et al.(Castro-Hernandez et al., 2011) to calculate the gas bubble diameter based on the ratio of the flows in a high-speed regime. The droplet generation frequency shows relatively less dependence on the dimensionless flow rate ratio (Fig. 8.10b). In general, however, f_d increases with φ in the dripping regime and decreases with φ in geometry-controlled mode. As reported by Anna and Mayer,(Anna and Mayer, 2006) transitions between the droplet formation regimes are weakly dependent on φ; rather, the capillary number plays a more determining role in controlling the mode of droplet breakup.

This study used low lipid flow rates (12–26 µL min^{-1}) and correspondingly low liquid perfluoropentane pressures in order to conserve fluids and better demonstrate the viability of highspeed droplet generation as a bulk manufacturing process. By comparison, Hettiarachchi et al.(Hettiarachchi et al., 2007b) supplied the lipid phase at rates between 30 and 120 µL min^{-1}. Based on the trends observed in Fig. 8.7b

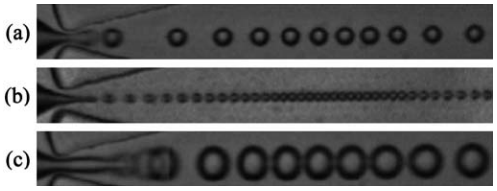

Figure 8.6: Representative images of three distinct droplet formation regimes. (a) Geometry-controlled. A series of overlaid images, successive in time, demonstrate the protrude-and-retract mechanism of the dispersed phase finger. (b) Dripping. Droplets break off from the tip of the dispersed phase finger at high rates due to ''steady'' Rayleigh capillary instability. (c) Jetting. A series of overlaid images, successive in time, demonstrate the break off of droplets due to ''dynamic'' Rayleigh capillary instability. The image height is 25 µm.

and 8.10b, even quicker droplet generation frequencies may be attained by increasing the continuous phase flow to further push the capillary number. As well, multiplexing numerous flow-focusing circuits to expand the number of droplet formation units, while maintaining device operation in the dripping regime, would scale the throughput. A 10x scale-up, for instance, would reduce the time to produce $1x10^9$ droplets— similar in scale to the amount of droplets formed by mechanical agitation, and well beyond the estimated $2x10^7$ monodisperse emulsions(Hettiarachchi et al., 2009) necessary for therapeutics in humans—from several hours to mere minutes.

Stability

We assessed a population of droplets with a mean diameter of 4.5 µm for size stability over a two-week time span. To our knowledge this study is the first to simulate an on-the-shelf environment by storing phase-change droplets at room temperature. Over two weeks the mean droplet diameter drifted less than 4%, from 4.5±0.2 µm to 4.3±0.3 µm (Fig. 8.11). It may be possible to prolong the shelf life beyond several weeks by modifying the poloxamer or PEG group, though unnecessary in practice considering

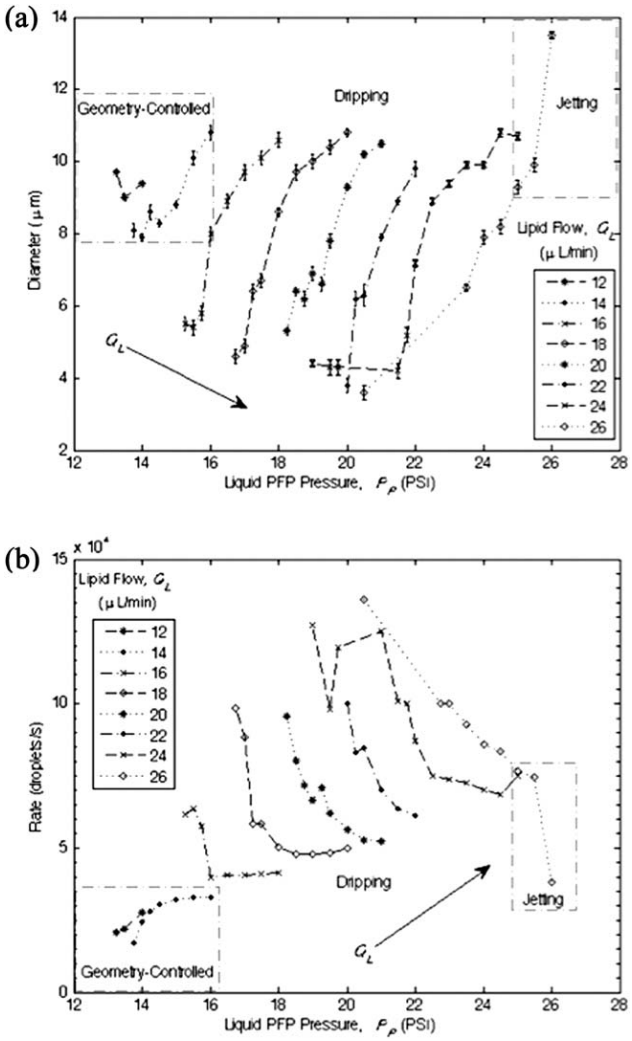

Figure 8.7: Diagrams of the production characteristics as determined by the flow parameters. Boxes distinguish geometry-controlled and jetting modes of droplet formation from dripping. (a) Droplet diameter D as a function of the lipid flow Q_L and the liquid perfluoropentane pressure P_P. (b) Generation frequency f_d as a function of Q_L and P_P.

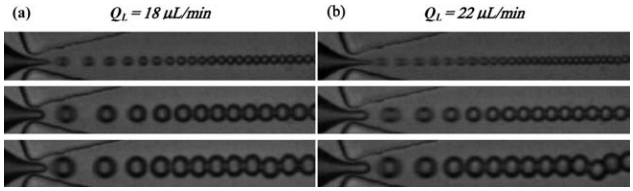

Figure 8.8: Sequence of images showing the effect of liquid perfluoropentane pressure for two lipid flows in the dripping regime. The droplet diameter decreases and the generation frequency quickens as the dimensionless flow rate ratio φ=Q_L/Q_P increases. (a) Q_L=18 µL min^{-1}. Top to bottom: P_P=17 psi, φ=55, D=4.9±0.2 µm, f_d=8.82x10^4 Hz; P_P=18 psi, φ=18, D=8.6±0.1 µm, f_d=5.04x10^4 Hz; P_P=19 psi, φ=9, D=10.0±0.2 µm, f_d=4.80x10^4 Hz. (b) Q_L=22 µL min^{-1}. Top to bottom: P_P=20 psi, φ=128, D=3.8±0.2 µm, f_d=1.00x10^5 Hz; P_P=21 psi, φ=20, D=7.9±0.1 µm, f_d=7.00x10^4 Hz; P_P=22 psi, φ=12, D=9.8±0.2 µm, f_d=6.12x10^4 Hz. The image height is 25 µm.

that clinical phase-change and contrast agents formed via mechanical agitation are injected immediately into the patient.

Thermal vaporization

The relatively low boiling point of liquid perfluoropentane (29°C) suggests spontaneous liquid-to-gas transition at body temperature; however, consistent with previous studies,(Kripfgans et al., 2000; Giesecke and Hynynen, 2003) encapsulation of the perfluorocarbon in a lipid shell increases the Laplace pressure sufficiently to stabilize the droplets well beyond the natural boiling point of pure liquid perfluoropentane. We observed rapid thermal vaporization of multiple droplet populations, collected at different days, at 88°C in a stirred waterbath. Droplets remain in a superheated state prior to this activation threshold.

As shown in Fig. 8.12, gas bubbles formed by vaporization expanded well beyond the volume predicted by the ideal gas law, PV=nRT, which approximates a volume expansion factor of 125[3](Kripfgans et al., 2000). Upon activation, 4.5±0.2 µm droplets initially converted into gas bubbles 106.7±4.6 µm in diameter, a diameter expansion of 24x. Kripfgans et al.(Kripfgans et al., 2000) detailed this further expansion as due to the intake of dissolved gases from the host fluid after conversion of the droplet to the gas bubble of pure perfluoropentane, an effect we have observed experimentally in our previous studies with perfluorocarbons.(Sheeran et al., 2011a) That the carrier fluid was not degassed prior to heating contributed to this large initial increase in size. Subsequent dissolution of these extra gases resulted in gas bubbles with a resting

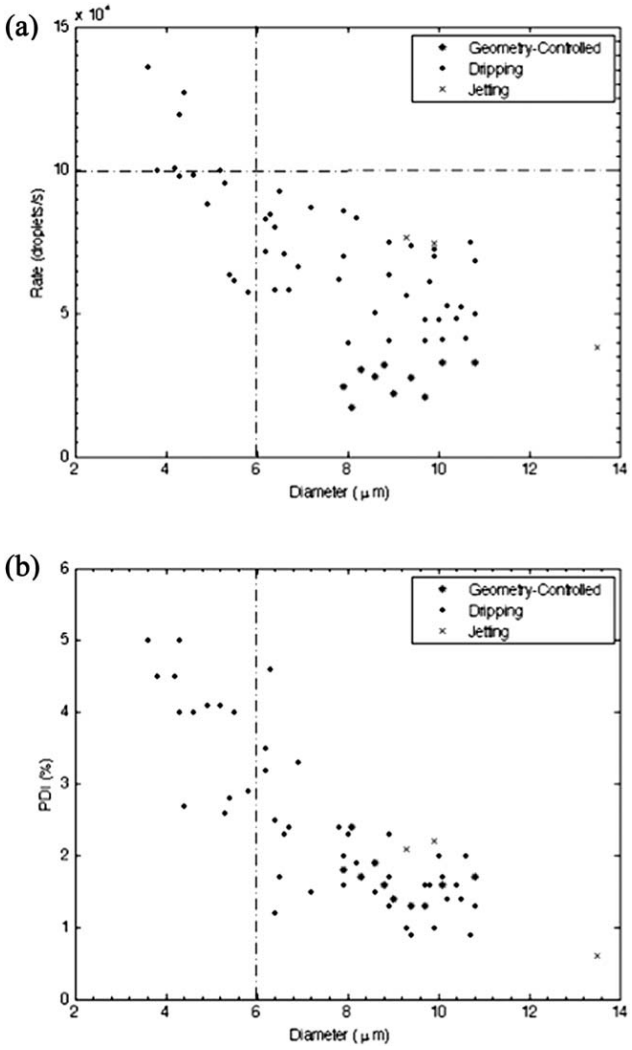

Figure 8.9: Plots relating the generation frequency and polydispersity index to droplet size. The dripping regime enables droplet formation in the appropriate 3–6 µm range at high frequency and monodispersity. (a) Generation frequency f_d as a function of droplet diameter D. (b) Polydispersity index (PDI) as a function of D. All flow conditions generated droplets with PDI $<5\%$.

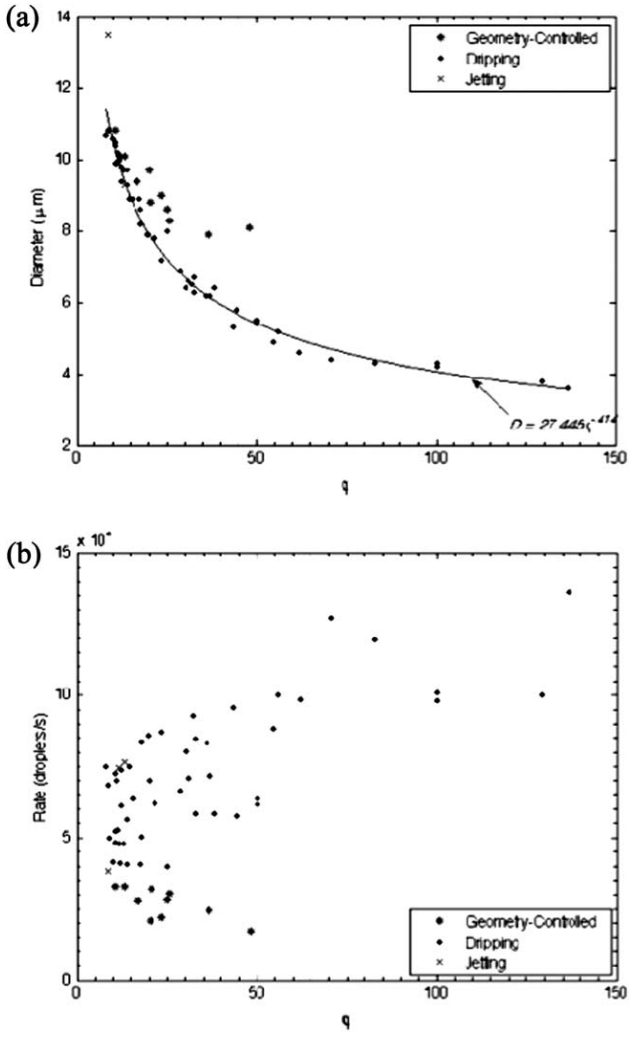

Figure 8.10: Diagrams of the production characteristics as determined by the ratio of the continuous lipid flow to the dispersed liquid perfluoropentane flow, $\varphi = Q_L/Q_P$. (a) The droplet diameter D as a function φ. For a given φ, droplet formation in geometry-controlled mode generates droplets of a larger size than in dripping mode. A power-series equation, valid in the dripping regime, emerges to predict droplet size based on the dimensionless flow rate ratio as $D = 27.445\varphi^{0.414}$ ($r^2 = 0.99$). (b) Generation frequency f_d as a function of φ. Increasing φ tends to slow f_d in geometrycontrolled mode and quicken f_d in dripping mode.

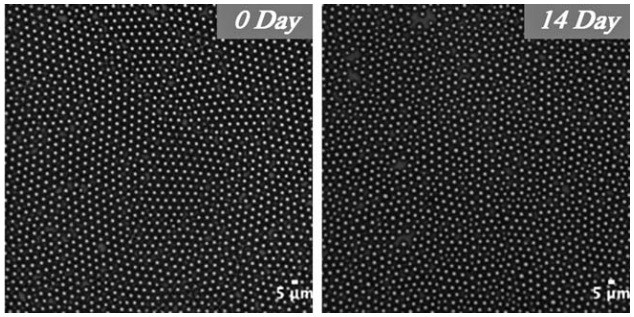

Figure 8.11: Images showing stability of a droplet population over a two-week time period. Droplets 4.5 µm in diameter drifted less than 4% in size over 14 days in a sealed glass vial at room temperature. Thus our phase-change droplets exhibited high stability in a true on-the-shelf setting. Scale bar represents 5 µm.

diameter of 27.4±1.2 µm, a 6x increase from the original droplet diameter, imaged several days after vaporization (Fig. 8.12, inset).

These experiments were repeated for vials containing pure liquid perfluoropentane and pure lipid solution. Under observation, pure liquid perfluoropentane transitioned directly to gas perfluoropentane, thus leaving an ''empty'' vial. Pure lipid solution boiled up to 120°C without the formation of gas bubbles.

The size stability of our droplets enabled consistent thermal activation of droplet populations stored at room temperature over two weeks. At threshold, droplet activation occurs in a near simultaneous manner. Likewise, we demonstrate in a parallel study that monodisperse droplets generated by our microfluidic device respond uniformly to acoustic pressure delivered from a 5 MHz piston transducer.(Martz et al., 2011) This parallel study confirms our initial hypothesis that acoustic droplet vaporization can be made homogeneous by the precision engineering of phase-change agents using microfluidics.

Consistent thermal and acoustic responses make these liquid perfluoropentane droplets ideal for targeted vessel occlusion to enhance HIFU, RFA, LA, and LITT in the treatment of cancers such as hepatocellular carcinomas, hepatic metastases, and renal cell carcinomas. The inclusion of an anti-cancer drug layer within the droplet may further potentiate these treatment modalities. Our device design lends itself to the inclusion of such a drug layer by combining a second hydrodynamic flow-focusing region at the droplet formation unit, as done in microbubble studies by Hettiarachchi et al.(Hettiarachchi et al., 2009) Chemoembolization—the addition of a chemotherapeutic agent—has been used to reduce perfusion and deliver therapeutics to treat

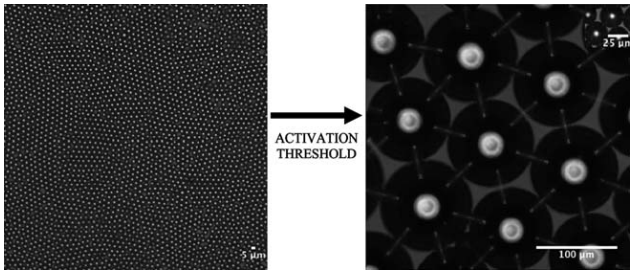

Figure 8.12: Thermal vaporization of a population of liquid perfluoropentane droplets after heating in a stirred water bath. Rapid droplet activation was observed at a water bath temperature of 88°C. Upon vaporization, 4.5 µm droplets initially transitioned into gas bubbles 106.7 µm in diameter. (Inset) Occlusive bubbles with a resting diameter of 27.4 µm resulted following dissolution of extra gases.

renal cell carcinoma alongside RFA(Arima et al., 2007) and hepatocellular carcinoma alongside RFA(Yamakado et al., 2009) and HIFU.(Wu et al., 2005) Besides forming polydisperse size distributions, conventional production techniques result in inconsistent drug dosages. Manufacturing utilizing microfluidics enables the accurate control of therapeutic payloads, and thus may improve localized drug delivery as well as thermal and acoustic responses. Further, adaptation of our microfluidic device to produce monodisperse double emulsions may enable the encapsulation of hydrophilic drugs such as thrombin(Fabiilli et al., 2010b) to extend the duration of occlusions generated by phase-change agents.

8.2.5 Conclusion

With microfluidics we can generate highly monodisperse phase-change droplets in the size range suitable for gas embolotherapy as a cancer treatment. By adjusting the flow rate of the contin- uous outer phase, we varied the capillary number and observed three distinct droplet formation regimes: traditional geometry- controlled mode, characterized by a protrude-and-retract mechanism of droplet break off; dripping, characterized by ‘‘steady’’ Rayleigh capillary instability; and jetting, characterized by ‘‘dynamic’’ Rayleigh capillary instability. Geometric optimization of the flow-focusing region and operation of the device in the dripping regime enabled the single-file generation of droplets at rates exceeding 10^5 Hz. To our knowledge this study is the first to report on the generation of clinical-scale quantities of droplet emulsions truly suitable for *in vivo* intravenous therapeutics.

For our flow-focusing device operated in the dripping regime, we can predict droplet diameter D_d based on the dimensionless ratio of the flow rates of the continuous outer phase Q_C and the dispersed inner phase Q_D. In simplified terms, we characterize our device in the dripping regime by $D_d \cong 27(Q_C/Q_D)^{-5/12}$.

Droplet populations generated by our microfluidic device are monodisperse, stable at room temperature, and transition uniformly to gas bubbles when presented with thermal and acoustic stimuli. Looking ahead, we aim to build a drug layer into our liquid perfluoropentane droplets to generate, using super high-speed microfluidics, phase-change droplets for gas chemoembolotherapy. Simultaneous delivery of a chemotherapeutic agent should elevate local concentrations of the drug with little escape to the systemic circulation due to vessel occlusion. Combining gas chemoembolotherapy with locoregional therapies such as thermal ablation and percutaneous ethanol injection presents a nice prospect to enhance heat and alcohol trapping and more effectively treat cancers.

8.2.6 Acknowledgements

The authors would like to thank Andrew Hatch and Robert Lin of our BioMint lab UC Irvine for discussions regarding this project. The National Institutes of Health, Grant #1 RO1 EB008733-01A1, provided funding for this work.

8.3 Microfluidic generation of acoustically active nanodroplets [3]

Thomas D. Martz[1], David Bardin[2], Paul S. Sheeran[3], Abraham Lee[2], and Paul A. Dayton[3*]

[1]Curriculum of Applied Science & Engineering - Material Science, University of North Carolina-North Carolina State University, Chapel Hill, NC, USA

[2]Department of Biomedical Engineering, University of California-Irvine, Irvine, California, USA

[3]Joint Dept. of Biomedical Engineering, University of North Carolina-North Carolina State University, Chapel Hill, NC, USA

Keywords: acoustic droplet vaporization, ultrasound, monodispersed, perfluorocarbon, phase-change

8.3.1 Introduction, Results, Discussion & Conclusion

Liquid perfluorocarbon droplets have emerged in medical acoustics as acoustically active particles for applications in embolization, contrast imaging, and targeted therapeutics. Acoustic droplet vaporization (ADV) occurs when the inner core of a perfluorocarbon droplet phase-shifts from the liquid state to the gas state as a result of an applied ultrasound pressure. Whereas the initial liquid droplet benefits from increased stability and small size, the resultant echogenic bubble can provide contrast to enhance ultrasound(Kripfgans et al., 2002) or can potentiate the delivery of therapeutics.(O'Neill and Rapoport,) The most common liquids of the droplet core, compounds in the perfluorocarbon family are non-toxic in small doses and inert, and, due to high molecular weights, are moderately stable in circulation.(Mattrey, 1994) While most ADV investigations have focused on droplets in the micron range for intravascular procedures, the field of medical ultrasound has shown recent interest in sub-micron liquid perfluorocarbon droplets for extravascular applications. Capitalizing on the characteristically 'leaky' vasculature of many solid tumors, sub-micron droplets may extravasate into the tumor interstitium through inter-endothelial gaps and accumulate(Campbell, 2006), or may be able to traverse the lymphatic system. Prior studies have shown sub-micron ADV agents to be useful in drug delivery(Rapoport et al., 2009b), enhanced thermal ablation(Zhang and Porter, 2010; Kawabata et al., 2005), and diagnostic imaging and

[3]Submitted to Small. Permission granted from T. D. Martz, D Bardin, P. S. Sheeran et al.

tissue characterization.(Martz et al., 2011; Kawabata et al., 2005; Sheeran, 2011; Asami et al., 2010) Rapoport et al.(Rapoport et al., 2009b) in particular demonstrated, *in vivo*, that paclitaxel-loaded droplets can be released with high spatial specificity, resulting in tumor regression. One main limitation of current methods is the use of processing techniques such as emulsification(Kawabata et al., 2005) and sonication(Mohan and Rapoport, 2010) to generate these nanodroplets, which result in polydisperse populations and significant variation in the reported activation threshold due to the strong correlation between vaporization energy and perfluorocarbon droplet size.(Martz et al., 2011; Sheeran et al., 2011b) Narrowing the size distribution would likely improve the biodistribution of sub-micron ADV agents, as well. Significant clinical motivation thus exists for a precise method to generate perfluorocarbon nanodroplets for use in extravascular tumor therapies.

Previously our group assessed the feasibility of microfluidic generation of ADV agents in the micron range to achieve precision control of droplet size and uniform activation. (Martz et al., 2011; Bardin et al., 2011) In this manuscript, we present a novel microfluidic system to generate engineered populations of *sub-micron* liquid perfluoropentane droplets for contrast-enhanced ultrasound imaging of the tumor interstitium. Compared with previous microfluidic systems to generate nanodroplets which relied on satellite droplet sorting(Tan and Lee, 2005) to produce droplets sizes as small as 100 nm, our system uses tip-streaming, made consistent with a pressure-controlled reagent delivery system and enhanced with the addition of a surfactant(Ward et al., 2010) to the continuous phase, to generate primary droplets of lipid-encapsulated perfluorocarbons as small as 360 nm, despite an orifice width of over an order of magnitude larger. Relative to satellite droplet sorting, advanced tip-streaming, as we demonstrate (Figure 8.13), allows for efficiency in generating droplets in the sub-micron range, without filtration or dynamic in-device separation.

By precisely varying the pressures and, consequently, the flow rates of the continuous and dispersed phases, we were able to produce narrowly dispersed lipid-encapsulated nano- and microdroplets ranging from 360 nanometers to 11 microns with the same microfluidic device (Table 8.3). Droplets larger than 1 micron were quantified with high-speed light microscopy as they exited the orifice. Production rates of 3.6±0.2, 6.8±0.2, and 11.8±0.3 micron droplets were 8.7, 4.0, and 3.2 x10^4 droplets/second, respectively. Smaller droplets could not be resolved with traditional light microscopy, and hence were collected and then assessed by dynamic light scattering with a Malvern Nanosizer (Figure 8.14) after production and thus production rate data was not obtained. TEM

of a number of the samples verified results of the Malvern Nanosizer (Figure 8.15).

In order to confirm the resulting samples were acoustically vaporizable, droplets were sonicated with 100 cycle pulses of varying amplitude at 3.2 MHz. As described by Sheeran et al (2011)(Sheeran et al., 2011a), the pressure required to vaporize droplets increases as droplet size decreases. In this study, a peak rarefactional pressure of approximately -3.15 MPa was sufficient to vaporize the majority of droplets in focus when the droplet size was greater than approximately 7 µm in diameter. As expected, smaller samples required substantially more pressure to vaporize. Droplets near 0.9 µm in diameter required approximately 4 MPa to vaporize, while smaller droplets could not be vaporized due to the maximum output limit of our ultrasound system (4.3 MPa peak rarefactional pressure). Activation thresholds established from these studies is in agreement with vaporization thresholds previously identified for individual perfluoropentane droplets.(Martz et al., 2011) That bulk droplet samples can be activated at pressures similar to the thresholds for individual droplets confirms one of the chief benefits of ADV droplet production through microfluidics – uniform activation.

Our results demonstrate that sub-micron (and micron) droplets for acoustic droplet vaporization applications can be effectively generated using droplet-based microfluidics. The pressure-controlled reagent delivery system crucially enabled the quick and precise tuning of the continuous and dispersed phases to maintain constant rates of flow and a consistent tip-streaming. By contrast, in our prior studies utilizing mechanical pumping, we were unable to maintain the tip-streaming of sub-micron droplets for sufficient time to collect samples. To our knowledge, this study is the one of the first examples of sub-micron production of primary encapsulated liquid droplets from a microfluidic device. The ability to achieve sub-micron droplet production, as well as the ability to produce droplet populations of uniform size, will have a significant impact in burgeoning medical applications requiring acoustically active nano- and microdroplets.

Average Diameter µm	Standard Deviation	Production Rate Droplets/sec.
0.36	0.05	*
0.85	0.15	*
3.6	0.2	8.7×10^4
6.8	0.2	4.0×10^4
11.7	0.3	3.2×10^4

Table 8.3: Average diameter, standard deviation, and production rate for perfluorocarbon droplets produced with microfluidic flow focusing.

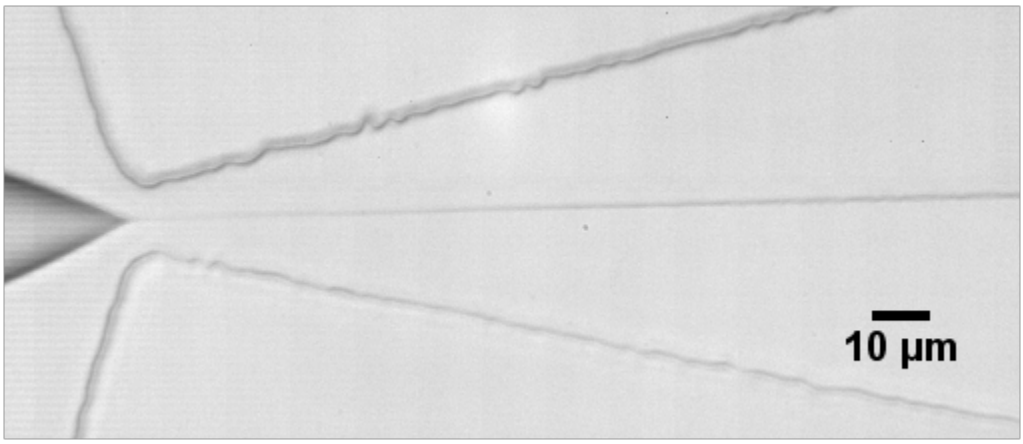

Figure 8.13: "Nano tipstreaming" of submicron droplets in a microfluidic device. Individual nanodroplets cannot be resolved by optical microscopy.

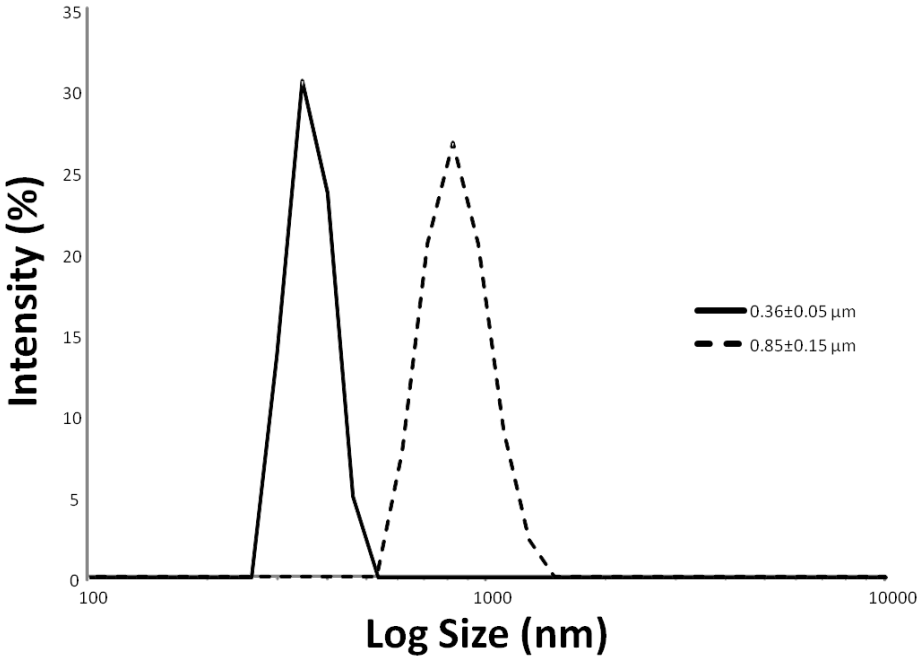

Figure 8.14: Particle size distribution, as reported by the Malvern Nanosizer, for 850 ± 150 nm population.

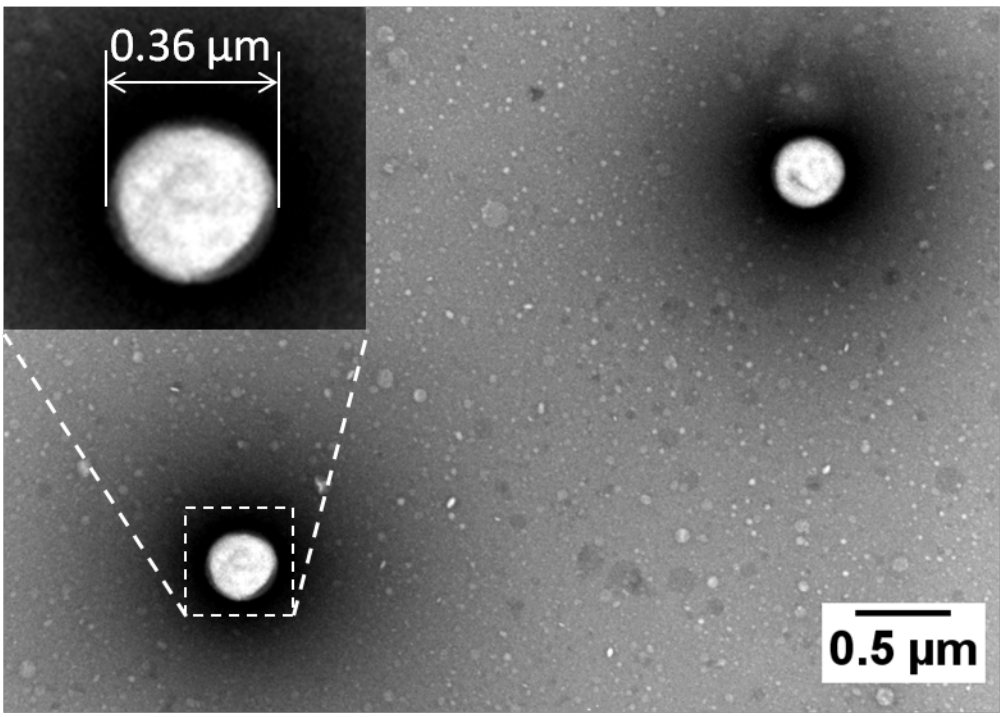

Figure 8.15: Transmission electron microscopy example of negative-stained perfluorocarbon droplets. Size measurement of 30 droplets indicated a distribution of 312 ± 49 nm.

8.3.2 Experimental Section

Reagent Preparation: The continuous phase lipid solution was prepared using a 9:1 molar ratio of 1,2-distearoyl-sn-glycero-3-phosphocoline (DSPC) (Avanti Polar Lipids, Alabaster, AL) and 1,2-distearoyl-sn-glycero-3-phosphoethanolamine-N[methoxy-(polyethylene glycol)-5000] (DSPE-PEG5000) (Avanti Polar Lipids, Alabaster, AL) in saline. Lipid solution was combined with glycerol (Fisher Scientific, Pittsburgh, PA) and Pluronic F-68 (Sigma Aldrich Corporation , St. Louis, MO) in a 1:1:1 mL volumetric ratio. Liquid perfluoropentane (FluoroMed, Round Rock, Texas) was utilized as the dispersed phase.

Microfluidic Device Fabrication: The process for developing the microfluidic wafer has been previously described by Hettiarachchi el al. (2009).(Hettiarachchi et al., 2009) Briefly, microfluidic channels were designed using Illustrator (Adobe, San Jose, CA) and printed at 20,000 dpi by CAD/Art Services (Brandon, OR). In a class 10,000 clean room, a silicon wafer spin-coated with a UV-curable epoxy (SU-8-25, MicroChem, Newton, MA) and exposed to UV light to develop the channels as a negative mold. Bulk polydimethylsiloxane (PDMS) (Dow Corning, Midland, MI) and a curing agent were cast over the wafer at a 10:1 ratio, and the mold was cured at 60°C for at least eight hours. Microfluidic chips were separated from the wafer and cleaned along with the glass slides (2947-75X25, Corning, Corning, NY) in a plasma cleaner (Harrick Plasma, Ithaca, NY). The device components were exposed to a plasma field under a controlled pressure of 500 millitorr for three minutes. Upon removal, the microfluidic channels and glass slide were joined, creating a sealed microfluidic device. Then the channels were filled with deionized water to stabilize the hydrophilic environment.

Optical Observations: The microfluidic device was secured to a moving stand on an inverted microscope (Olympus 1X71 microscope, Center Valley, PA) with a 50X NA = 1.0 objective. A high-speed camera (FastcamAPX-RS, Photron, Inc., San Diego, CA) was used to capture images and videos of the device output.

Pressure Control Flow System: The reagent pump system was established in a similar manner to Korczyk.(Korczyk et al., 2010) The pressure to control the flow system was supplied by a compressed nitrogen tank with precision regulators for both the continuous and discontinuous flows. Each reagent vial had two holes in the septum, which were fed by Tygon S-54-HL tubing (Saint-Gobain Performance Plastics, Akron, OH). One tube was placed in the headspace that was connected to the pressure regulation system. The second tube was immersed in the reagent, which transferred the reagent

to the microfluidic device. The system was allowed to stabilize for one minute after pressure changes before sample collection began.

Optical Imaging and Sizing: Dimensions of the final microfluidic device were determined using Image J (NIH, Bethesda, Maryland) and a calibrated slide reticule (Edmund Optics, Barrington NJ). The orifice was 12 µm, the PFP channel was 46 µm, the lipid solution channel was 45 µm, and the filter spacing was 23 µm.

For micron sized droplets, diameter was determined optically as described for measurements of the microfluidic chip. Sub-micron droplets could not be resolved optically, and were instead collected in a pipette tip for light scattering or electron microscopy analysis.

Dynamic Light Scattering Sizing: A Malvern Nano ZS (Malvern Instruments Ltd., Malvern, Worcestershire, U.K.) was used to size droplets in the sub-micron diameter range. Sub-micron samples were diluted with 0.5 mL of phosphate buffered saline and placed into a cuvet for testing. Debris less than 100 nm were assumed to be lipid micelles.

Transmission Electron Microscopy (TEM) and Sizing: To verify the presence of perfluorocarbon droplets and corroborate Malvern sizing data, a negative staining procedure was used along with a TEM (Philips Tecnai 120kV, Amsterdam, The Netherlands). The negative staining first consisted of plasma treating the individual TEM grids for 90 seconds. 10 µl of the droplet sample was transferred via pipette onto the TEM grid and allowed to sit for 120 seconds. The TEM grid was dipped in a bath of 1% uranyl acetate for 60 seconds, and allowed to dry prior to TEM imaging.

Acoustic Droplet Vaporization: To verify that the generated droplet samples could be vaporized, a procedure similar to that described in Sheeran et al.(Sheeran, 2011) was utilized. In brief, a 3.2 MHz transducer with a focal length of 3.45 cm was used to activate the droplets in a cellulose tube submerged in a water bath at 37°C. Droplets within the optical focus were subjected to manually-triggered 100 cycle pulses with 1-2 seconds of rest between each trigger. Pressure was increased in steps of approximately 0.15 MPa until the pressure was sufficient to vaporized the majority (approximately 90% or greater) of the droplets in focus.

8.3.3 Acknowledgements

The authors would like to thank Jason Streeter for producing the initial lipid composition and Roger Shih for creation of the microfluidic wafer. We appreciate the

intellectual contributions of Dr. Terry Matsunaga on medical uses and formulation methods for perfluorocarbon droplets. This grant was supported by R01EB008733 and R21EB011704.

Bibliography

Anna, S. and Mayer, H. (2006). Microscale tipstreaming in a microfluidic flow focusing device. *Physics of Fluids*, 18(12):–. 121LD Times Cited:50 Cited References Count:51.

Apfel, R. (1998). Activatable infusable dispersions containing drops of a superheated liquid for methods of therapy and diagnosis. 5,840,276(08/780,337).

Arima, K., Yamakado, K., Kinbara, H., Nakatsuka, A., Takeda, K., and Sugimura, Y. (2007). Percutaneous radiofrequency ablation with transarterial embolization is useful for treatment of stage 1 renal cell carcinoma with surgical risk: results at 2-year mean follow up. *Int J Urol*, 14(7):585–90; discussion 590.

Asami, R., Ikeda, T., Azuma, T., Umemura, S., and Kawabata, K. (2010). Acoustic signal characterization of phase change nanodroplets in tissue-mimicking phantom gels. *Japanese Journal of Applied Physics*, 49(7).

Bardin, D., Martz, T., Sheeran, P., Shih, R., Dayton, P., and Lee, A. (2011). High-speed, clinical-scale microfluidic generation of stable phase-change droplets for gas embolotherapy. *Lab Chip*.

Campbell, R. (2006). Tumor physiology and delivery of nanopharmaceuticals. *Anti-cancer Agents Med Chem*, 6(6):503–12.

Castro-Hernandez, E., van Hoeve, W., Lohse, D., and Gordillo, J. (2011). Microbubble generation in a co-flow device operated in a new regime. *Lab Chip*, 11(12):2023–9.

Cubaud, T. and Mason, T. (2008). Capillary threads and viscous droplets in square microchannels. *Physics of Fluids*, 20(5):11.

Fabiilli, M., Haworth, K., Fakhri, N., Kripfgans, O., Carson, P., and Fowlkes, J. (2009). The role of inertial cavitation in acoustic droplet vaporization. *Ieee T Ultrason Ferr*, 56(5):1006–1017. 435VO Times Cited:9 Cited References Count:34.

Fabiilli, M., Haworth, K., Sebastian, I., Kripfgans, O., Carson, P., and Fowlkes, J. (2010a). Delivery of chlorambucil using an acoustically-triggered perfluoropentane emulsion. *Ultrasound Med Biol*, 36(8):1364–75.

Fabiilli, M., Lee, J., Kripfgans, O., Carson, P., and Fowlkes, J. (2010b). Delivery of water-soluble drugs using acoustically triggered perfluorocarbon double emulsions. *Pharm Res*, 27(12):2753–65.

Garstecki, P., Gitlin, I., DiLuzio, W., Whitesides, G., Kumacheva, E., and Stone, H. (2004). Formation of monodisperse bubbles in a microfluidic flow-focusing device. *Applied Physics Letters*, 85(13):2649–2651. 858FS Times Cited:197 Cited References Count:24.

Garstecki, P., Stone, H., and Whitesides, G. (2005). Mechanism for flow-rate controlled breakup in confined geometries: a route to monodisperse emulsions. *Phys Rev Lett*, 94(16):164501.

Giesecke, T. and Hynynen, K. (2003). Ultrasound-mediated cavitation thresholds of liquid perfluorocarbon droplets in vitro. *Ultrasound Med Biol*, 29(9):1359–65.

Goode, J. and Matson, M. (2004). Embolisation of cancer: what is the evidence? *Cancer Imaging*, 4(2):133–41.

Haworth, K., Fowlkes, J., Carson, P., and Kripfgans, O. (2008). Towards aberration correction of transcranial ultrasound using acoustic droplet vaporization. *Ultrasound Med Biol*, 34(3):435–45.

Hettiarachchi, K., Talu, E., Longo, M., Dayton, P., and Lee, A. (2007a). On-chip generation of microbubbles as a practical technology for manufacturing contrast agents for ultrasonic imaging. *Lab Chip*, 7(4):463–8.

Hettiarachchi, K., Talu, E., Longo, M. L., Dayton, P. A., and Lee, A. P. (2007b). On-chip generation of microbubbles as a practical technology for manufacturing contrast agents for ultrasonic imaging. *Lab Chip*, 7(4):463–8.

Hettiarachchi, K., Zhang, S., Feingold, S., Lee, A., and Dayton, P. (2009). Controllable microfluidic synthesis of multiphase drug-carrying lipospheres for site-targeted therapy. *Biotechnol Prog*, 25(4):938–45.

Huh, D., Bahng, J., Ling, Y., Wei, H., Kripfgans, O., Fowlkes, J., Grotberg, J., and Takayama, S. (2007). Gravity-driven microfluidic particle sorting device with hydrodynamic separation amplification. *Anal Chem*, 79(4):1369–76.

Kalman, D. and Varenhorst, E. (1999). The role of arterial embolization in renal cell carcinoma. *Scand J Urol Nephrol*, 33(3):162–70.

Kawabata, K., Sugita, N., Yoshikawa, H., Azuma, T., and Umemura, S. (2005). Nanoparticles with multiple perfluorocarbons for controllable ultrasonically induced phase shifting. *Japanese Journal of Applied Physics Part 1-Regular Papers Brief Communications & Review Papers*, 44(6B):4548–4552.

Kaya, M., Feingold, S., Hettiarachchi, K., Lee, A., and Dayton, P. (2010). Acoustic responses of monodisperse lipid-encapsulated microbubble contrast agents produced by flow focusing. *Bubble Sci Eng Technol*, 2(2):33–40.

Kobayashi, I., Uemura, K., and Nakajima, M. (2007). Formulation of monodisperse emulsions using submicron-channel arrays. *Colloids and Surfaces a-Physicochemical and Engineering Aspects*, 296(1-3):285–289.

Korczyk, P., Cybulski, O., Makulska, S., and Garstecki, P. (2010). Effects of unsteadiness of the rates of flow on the dynamics of formation of droplets in microfluidic systems. *Lab Chip*, 11(1):173–5.

Kripfgans, O., Fabiilli, M., Carson, P., and Fowlkes, J. (2004). On the acoustic vaporization of micrometer-sized droplets. *J Acoust Soc Am*, 116(1):272–81.

Kripfgans, O., Fowlkes, J., Miller, D., Eldevik, O., and Carson, P. (2000). Acoustic droplet vaporization for therapeutic and diagnostic applications. *Ultrasound Med Biol*, 26(7):1177–89.

Kripfgans, O., Fowlkes, J., Woydt, M., Eldevik, O., and Carson, P. (2002). In vivo droplet vaporization for occlusion therapy and phase aberration correction. *IEEE Trans Ultrason Ferroelectr Freq Control*, 49(6):726–38.

Kripfgans, O., Orifici, C., Carson, P., Ives, K., Eldevik, O., and Fowlkes, J. (2005). Acoustic droplet vaporization for temporal and spatial control of tissue occlusion: A kidney study. *Ieee T Ultrason Ferr*, 52(7):1101–1110. 954WV Times Cited:15 Cited References Count:17.

Lo, A., Kripfgans, O., Carson, P., and Fowlkes, J. (2006). Spatial control of gas bubbles and their effects on acoustic fields. *Ultrasound Med Biol*, 32(1):95–106.

Lo, A., Kripfgans, O., Carson, P., Rothman, E., and Fowlkes, J. (2007). Acoustic droplet vaporization threshold: effects of pulse duration and contrast agent. *IEEE Trans Ultrason Ferroelectr Freq Control*, 54(5):933–46.

Malloggi, F., Pannacci, N., Attia, R., Monti, F., Mary, P., Willaime, H., Tabeling, P., Cabane, B., and Poncet, P. (2010). Monodisperse colloids synthesized with nanofluidic technology. *Langmuir*, 26(4):2369–2373. 553CK Times Cited:7 Cited References Count:37.

Marsh, J., Partlow, K., Abendschein, D., Scott, M., Lanza, G., and Wickline, S. (2007). Molecular imaging with targeted perfluorocarbon nanoparticles: quantification of the concentration dependence of contrast enhancement for binding to sparse cellular epitopes. *Ultrasound Med Biol*, 33(6):950–8.

Martz, T., Sheeran, P., Bardin, D., Lee, A., and Dayton, P. (2011). Precision manufacture of perfluorocarbon droplets for acoustic droplet vaporization. *Ultrasound in Medicine and Biology*.

Mattrey, R. (1994). The potential role of perfluorochemicals (pfcs) in diagnostic imaging. *Artif Cells Blood Substit Immobil Biotechnol*, 22(2):295–313.

Miller, D., Averkiou, M., Brayman, A., Everbach, E., Holland, C., Wible, J., and Wu, J. (2008). Bioeffects considerations for diagnostic ultrasound contrast agents. *J Ultrasound Med*, 27(4):611–32; quiz 633–6.

Mohan, P. and Rapoport, N. (2010). Doxorubicin as a molecular nanotheranostic agent: effect of doxorubicin encapsulation in micelles or nanoemulsions on the ultrasound-mediated intracellular delivery and nuclear trafficking. *Mol Pharm*, 7(6):1959–73.

Nisisako, T. and Torii, T. (2008). Microfluidic large-scale integration on a chip for mass production of monodisperse droplets and particles. *Lab Chip*, 8(2):287–93.

Nisisako, T., Torii, T., and Higuchi, T. (2002). Droplet formation in a microchannel network. *Lab Chip*, 2(1):24–6.

O'Neill, B. and Rapoport, N. Phase-shift, stimuli-responsive drug carriers for targeted delivery. *Ther Deliv*, 2(9):1165–1187.

Quay, S. (1998). Phase shift colloids as ultrasound contrast agents. (2):1277.

Rapoport, N., Christensen, D., Kennedy, A., and Nam, K. (2010). Cavitation properties of block copolymer stabilized phase-shift nanoemulsions used as drug carriers. *Ultrasound in Medicine and Biology*, 36(3):419–429. 600TS Times Cited:1 Cited References Count:42.

Rapoport, N., Efros, A., Christensen, D., Kennedy, A., and Nam, K. (2009a). Microbubble generation in phase-shift nanoemulsions used as anticancer drug carriers. *Bubble Sci Eng Technol*, 1(1-2):31–39.

Rapoport, N., Gao, Z., and Kennedy, A. (2007). Multifunctional nanoparticles for combining ultrasonic tumor imaging and targeted chemotherapy. *J Natl Cancer Inst*, 99(14):1095–106.

Rapoport, N., Kennedy, A., Shea, J., Scaife, C., and Nam, K. (2009b). Controlled and targeted tumor chemotherapy by ultrasound-activated nanoemulsions/microbubbles. *J Control Release*, 138(3):268–76.

Schad, K. and Hynynen, K. (2010). In vitro characterization of perfluorocarbon droplets for focused ultrasound therapy. *Phys Med Biol*, 55(17):4933–47.

Sheeran, P. (2011). Phase-change contrast agents for imaging and therapy. *Current Pharmaceutical Design*.

Sheeran, P., Dayton, P., Wong, V., Luois, S., McFarland, R., Ross, W., Feingold, S., and Matsunaga, T. (2011a). Decafluorobutane as a phase-change contrast agent for low-energy extravascular ultrasonic imaging. *Ultrasound in Medicine and Biology*, 37(9):1518–1530. 801OK Times Cited:0 Cited References Count:48.

Sheeran, P., Luois, S., Dayton, P., and Matsunaga, T. (2011b). Formulation and acoustic studies of a new phase-shift agent for diagnostic and therapeutic ultrasound. *Langmuir*, 27(17):10412–20.

Talu, E., Hettiarachchi, K., Powell, R. L., Lee, A. P., Dayton, P. A., and Longo, M. L. (2008). Maintaining monodispersity in a microbubble population formed by flow-focusing. *Langmuir*, 24(5):1745–9.

Talu, E., Hettiarachchi, K., Zhao, S., Powell, R. L., Lee, A. P., Longo, M. L., and Dayton, P. A. (2007). Tailoring the size distribution of ultrasound contrast agents: possible method for improving sensitivity in molecular imaging. *Mol Imaging*, 6(6):384–92.

Tan, Y., Cristini, V., and Lee, A. (2006). Monodispersed microfluidic droplet generation by shear focusing microfluidic device. *Sensors and Actuators B-Chemical*, 114(1):350–356.

Tan, Y., Fisher, J., Lee, A., Cristini, V., and Lee, A. (2004). Design of microfluidic channel geometries for the control of droplet volume, chemical concentration, and sorting. *Lab Chip*, 4(4):292–8.

Tan, Y. and Lee, A. (2005). Microfluidic separation of satellite droplets as the basis of a monodispersed micron and submicron emulsification system. *Lab Chip*, 5(10):1178–83.

Teh, S., Lin, R., Hung, L., and Lee, A. (2008). Droplet microfluidics. *Lab Chip*, 8(2):198–220. 256VN Times Cited:307 Cited References Count:269.

Ward, T., Faivre, M., and Stone, H. (2010). Drop production and tip-streaming phenomenon in a microfluidic flow-focusing device via an interfacial chemical reaction. *Langmuir*, 26(12):9233–9.

Whitesides, G. (2006). The origins and the future of microfluidics. *Nature*, 442(7101):368–73.

Wu, F., Wang, Z., Chen, W., Zou, J., Bai, J., Zhu, H., Li, K., Jin, C., Xie, F., and Su, H. (2005). Advanced hepatocellular carcinoma: treatment with high-intensity focused ultrasound ablation combined with transcatheter arterial embolization. *Radiology*, 235(2):659–67.

Xia, Y. and Whitesides, G. (1998). Soft lithography. *Annual Review of Materials Science*, 28:153–184.

Xu, J., Li, S., Tan, J., Wang, Y., and Luo, G. (2006). Controllable preparation of monodisperse o/w and w/o emulsions in the same microfluidic device. *Langmuir*, 22(19):7943–6.

Yamakado, K., Anai, H., Takaki, H., Sakaguchi, H., Tanaka, T., Kichikawa, K., and Takeda, K. (2009). Adrenal metastasis from hepatocellular carcinoma: radiofrequency ablation combined with adrenal arterial chemoembolization in six patients. *AJR Am J Roentgenol*, 192(6):W300–5.

Zhang, M., Fabiilli, M., Haworth, K., Fowlkes, J., Kripfgans, O., Roberts, W., Ives, K., and Carson, P. (2010). Initial investigation of acoustic droplet vaporization for occlusion in canine kidney. *Ultrasound Med Biol*, 36(10):1691–703.

Zhang, M., Fabiilli, M., Haworth, K., Padilla, F., Swanson, S., Kripfgans, O., Carson, P., and Fowlkes, J. (2011). Acoustic droplet vaporization for enhancement of thermal ablation by high intensity focused ultrasound. *Academic Radiology*, 18(9):1123–1132. 812GJ Times Cited:0 Cited References Count:56.

Zhang, P. and Porter, T. (2010). An in vitro study of a phase-shift nanoemulsion: a potential nucleation agent for bubble-enhanced hifu tumor ablation. *Ultrasound Med Biol*, 36(11):1856–66.